

Computer-aided Analysis of Endoscopic-frames for the Detection of Abnormalities in Gastrointestinal Tract

Hussam Ali
CIIT/SP15-PCS-005/WAH

Research Collaborator: Mubashir Husain Rehmani

Outline



- 1. Introduction**
- 2. Literature Review**
- 3. Challenges**
- 4. Problem Statement**
- 5. Proposed Methods**
- 6. Results and Discussions**
- 7. Conclusion and Future Work**
- 8. Contributions**
- 9. References**
- 10. Questions Answers**



Outline



- 1. Introduction**
- 2. Literature Review**
- 3. Challenges**
- 4. Problem Statement**
- 5. Proposed Methods**
- 6. Results and Discussions**
- 7. Conclusion and Future Work**
- 8. Contributions**
- 9. References**
- 10. Questions Answers**



Introduction



Statistics

- Every year nearly 1 million cases of gastric cancer are reported.
- Due to gastric abnormalities more than 0.7 million deaths are recorded worldwide every year.
- Worst conditions are in less developed countries (e.g., Middle East and Asian countries) .

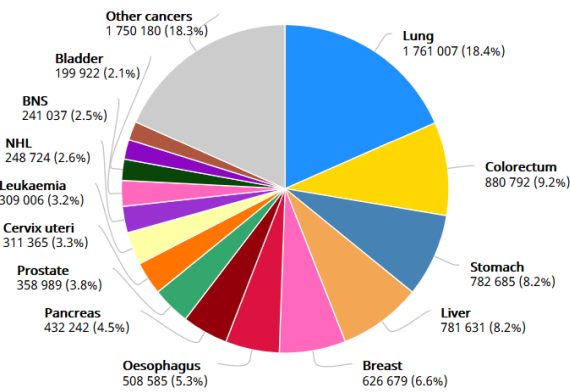
W. H. Organization. (2019, 10/02/2020). Stomach fact sheet Available:
<http://gco.iarc.fr/today/data/factsheets/cancers/7-Stomach-fact-sheet.pdf>



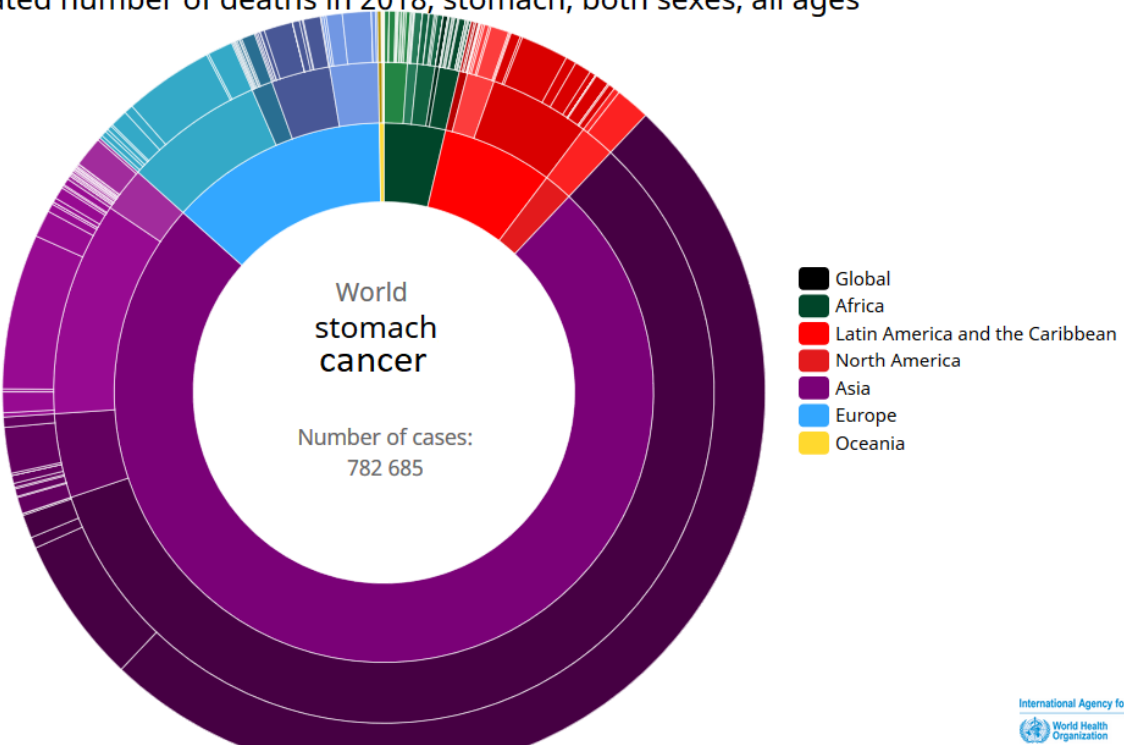
Introduction



Statistics



Estimated number of deaths in 2018, stomach, both sexes, all ages



International Agency for Research on Cancer
World Health Organization

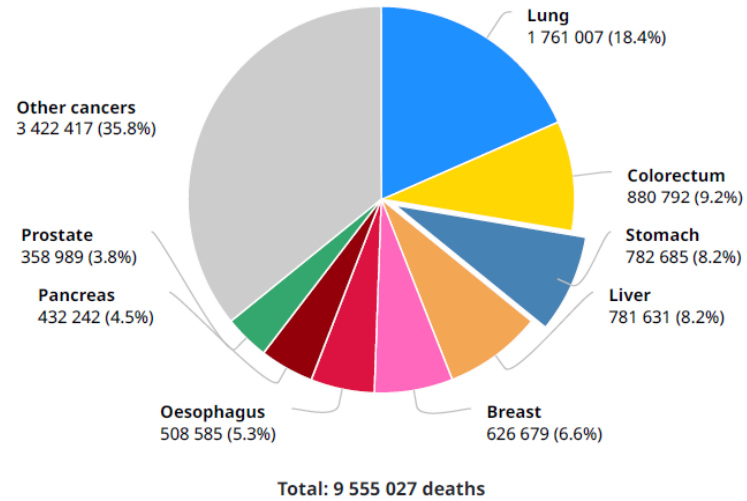
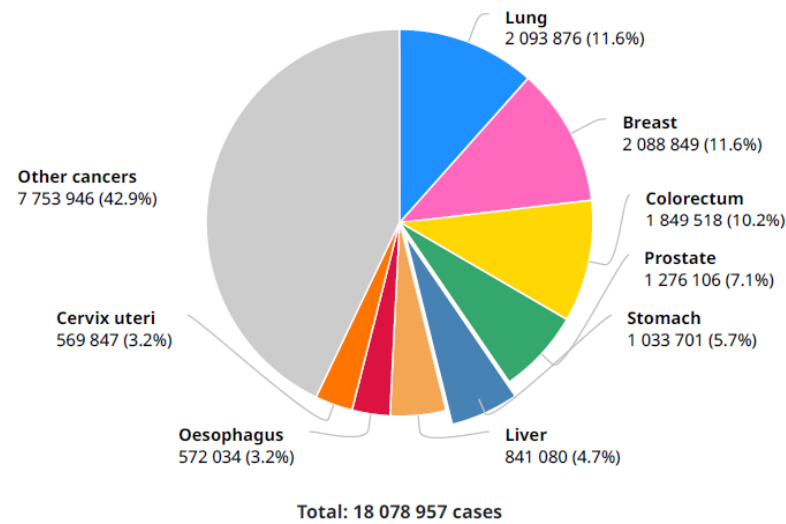
W. H. Organization. (2019, 10/02/2020). Stomach fact sheet Available:
<http://gco.iarc.fr/today/data/factsheets/cancers/7-Stomach-fact-sheet.pdf>



Introduction



Statistics



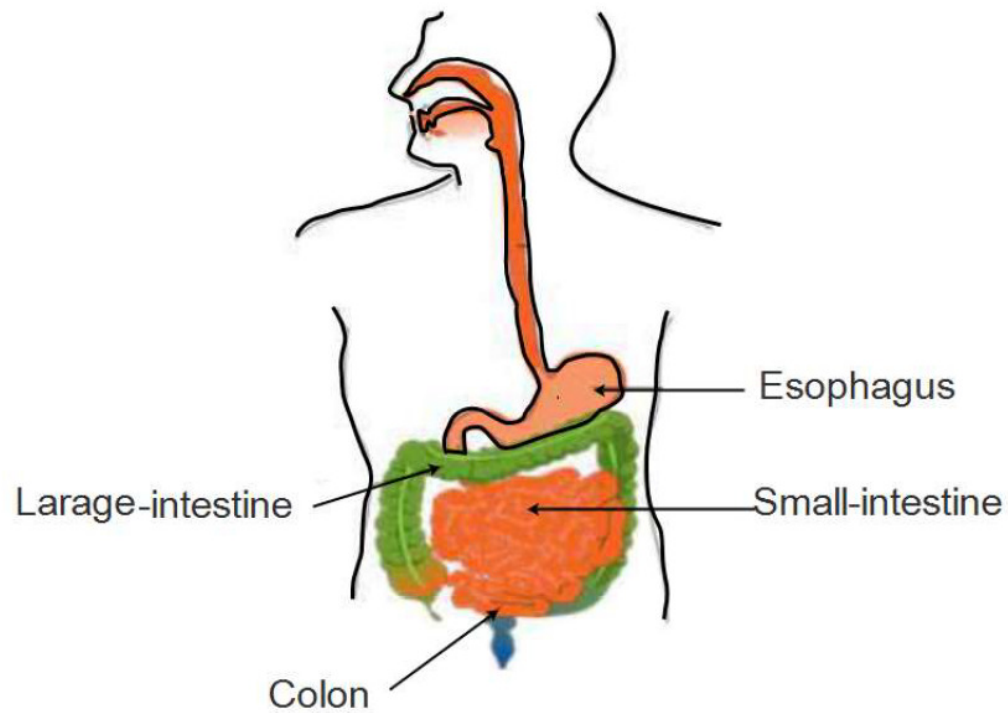
W. H. Organization. (2019, 10/02/2020). stomach cancer fact sheet Available:
<http://gco.iarc.fr/today/data/factsheets/cancers/7-Stomach-fact-sheet.pdf>





Introduction

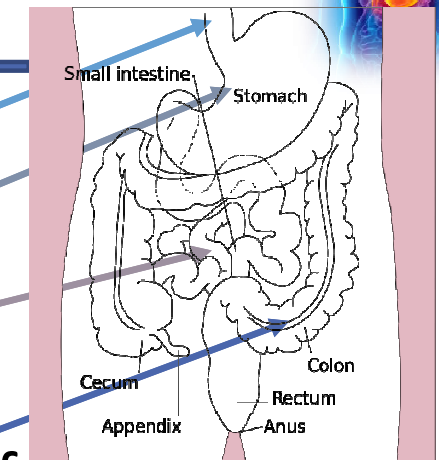
Anatomy



Pathology of Gastrointestinal

Gastrointestinal-Tract of a human having parts.

- **Esophagus:** Food first goes to esophagus.
- **Stomach:** Intestinal juice mixed with food.
- **Small Intestine:** Then food goes to the entrance of Small-intestine called duodenum.
- **Colon:** It is the last portion of GI tract and the most prone area for having tumors or polyps .



Structure of GI-tract [9-14]



Introduction



Screening and Diagnosis

Minimally Invasive

- Endoscopy is a less invasive method for screening gastrointestinal tract.
- Endoscope is a wire like instrument, a camera and light source attached to its distal tip.
- Sometimes used for biopsy by employing instrument channel.

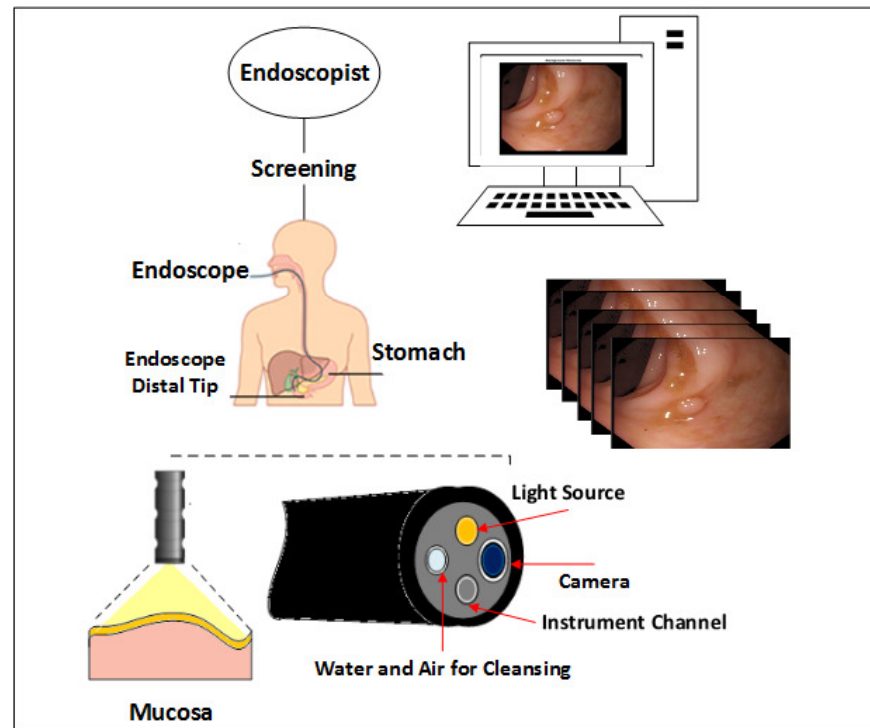
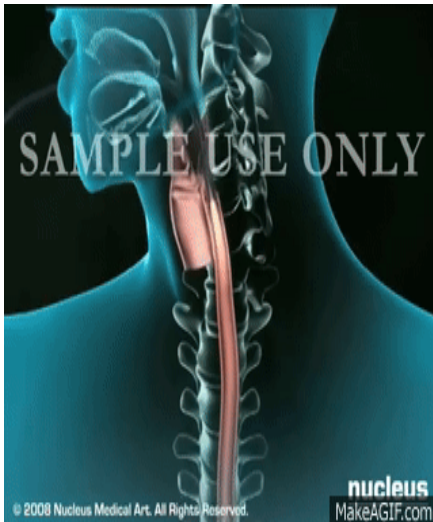
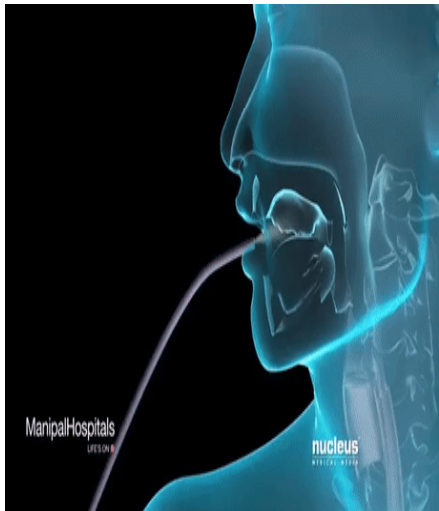




Introduction

Screening and Diagnosis

Image Acquisition and Setup for Endoscopic Screening



https://www.youtube.com/watch?v=_qrbzpDA98g

Computer-aided Analysis of Endoscopic-frames for the
Detection of Abnormalities in Gastrointestinal Tract

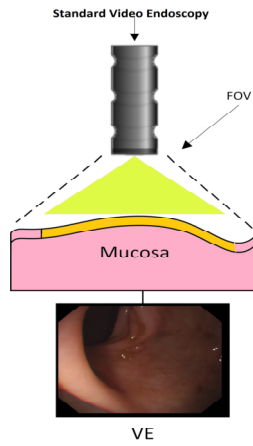


Types of Endoscopy



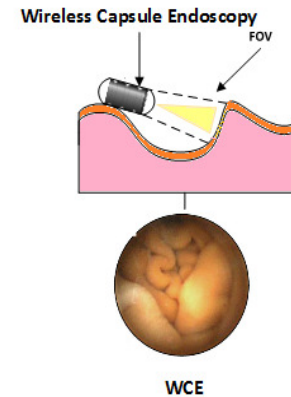
Wired Video Endoscopy (VE)

Endoscopy is a procedure which is performed by a flexible wire like instrument having mounted camera and light source.



Wireless Capsule Endoscopy (WCE)

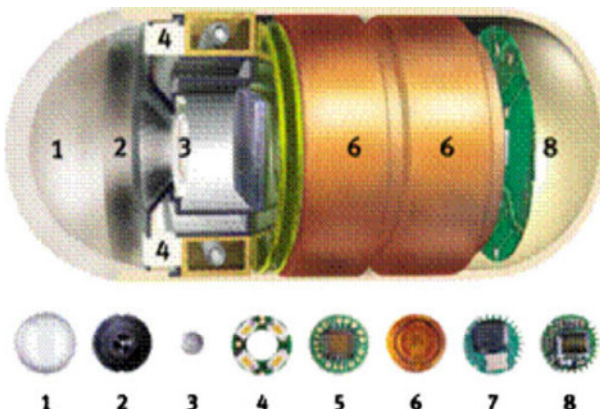
There are some areas e.g., small bowel that are unreachable from VE, so WCE is less invasive option for such cases.





Introduction

WCE



The components diagram of CE. (1) Optical dome, (2) lens holder (3), lens (4) illuminating LEDs, (5) CMOS imager, (6) battery, (7) ASIC RF transmitter, (8) antenna.



Introduction



■ Motivation

- Endoscopy procedure takes 45 minutes to 8 hours.
- After endoscopic procedure more than 50000 frames are produced.
- Difficult and lengthy process for a doctor to observe each frame

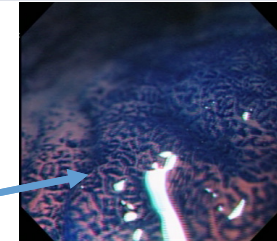


Stomach Cancer and Abnormalities



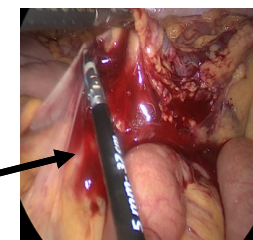
Some Examples of Abnormalities

■ **Cancer:** Start from unusual growth of cells [17-18].



Cancer (CH frame)

■ **Bleeding:** Bleeding is caused by cancer, Crohn's disease, or Hepatitis C [18-19].



Bleeding (VE frame)

■ **Polyps:** Polyps is unusual mucosal growth, and typically benign[19-20].



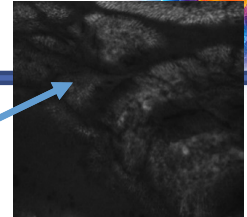
Polyp (VE frame)



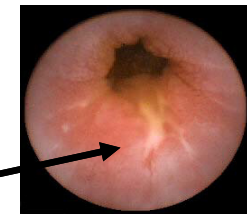
Stomach Cancer and Abnormalities

Some Examples of Abnormalities

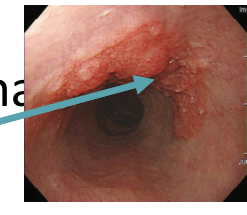
- **Celiac Disease:** This is an auto immune disorder in small intestine, the intolerance of gluton found in wheat.
- **Ulcer:** The ulcer is also referred as a disease that is caused by the acid produced by the stomach itself.
- **Inflammation:** Dyspepsia and acid reflex are associated with the inflammatory gastric lining .
The main cause of inflammation of gastritis is H. Pylori.



Celiac Disease



Ulcer WCE



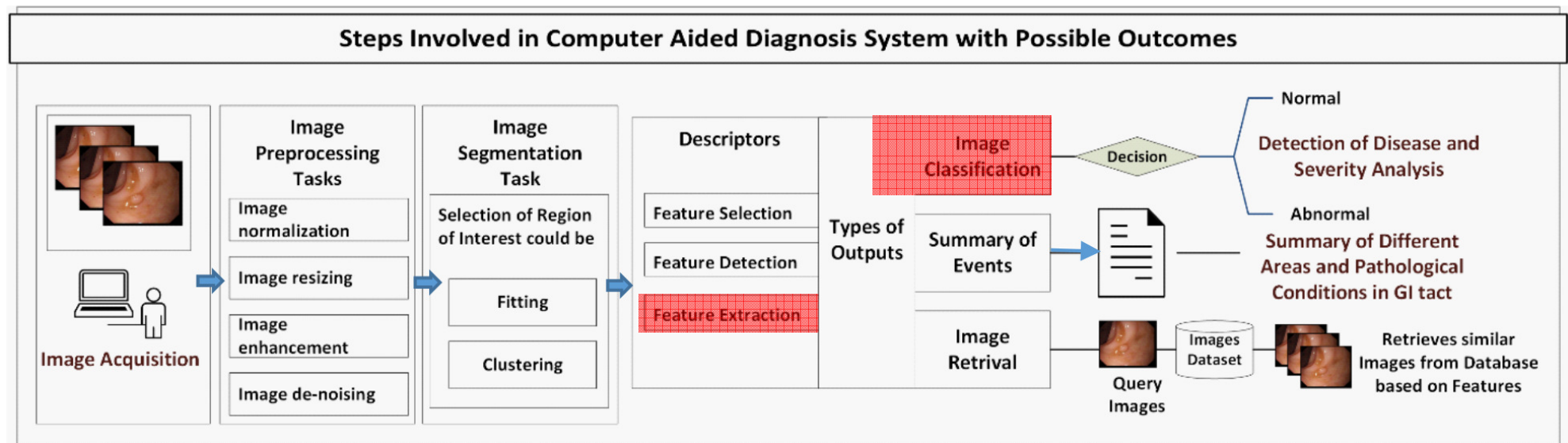
Inflammation



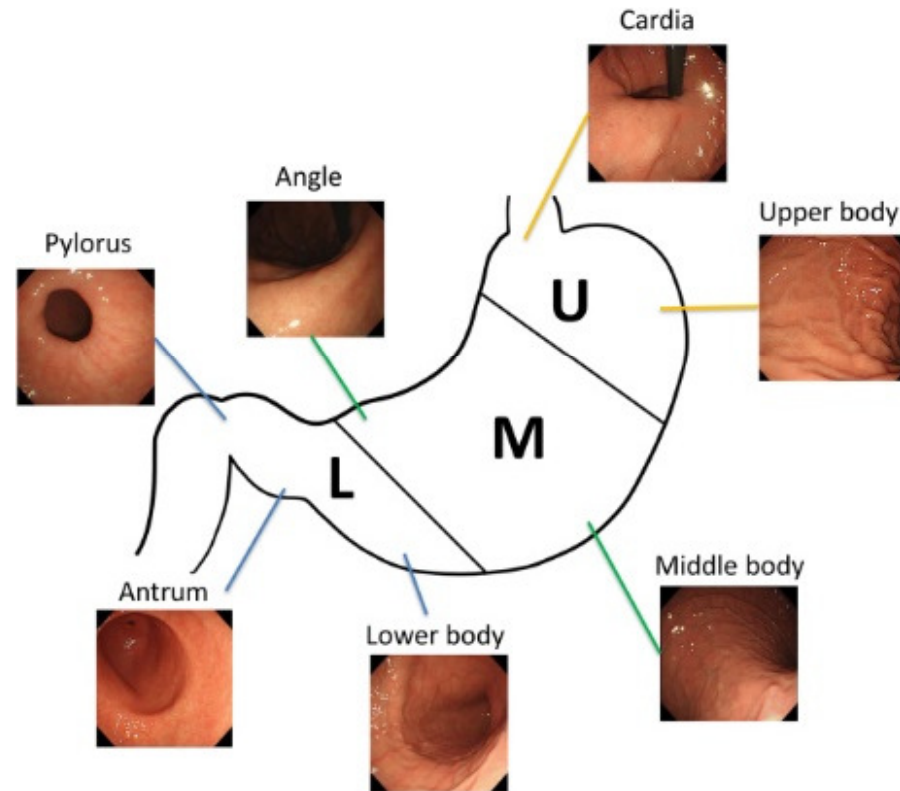
Introduction



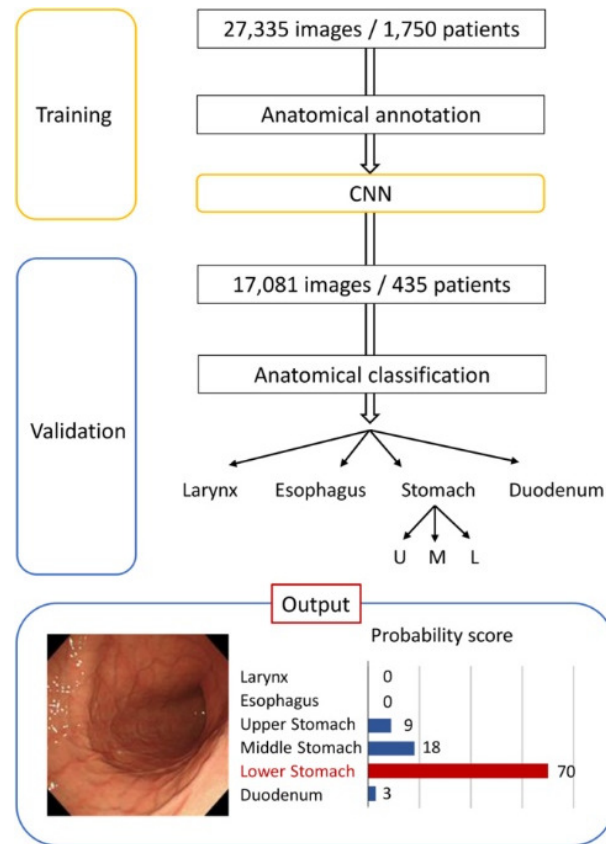
Computer-aided diagnosis for gastric patients is potential solution



Computer-aided Diagnosis System



Computer-aided Diagnosis System



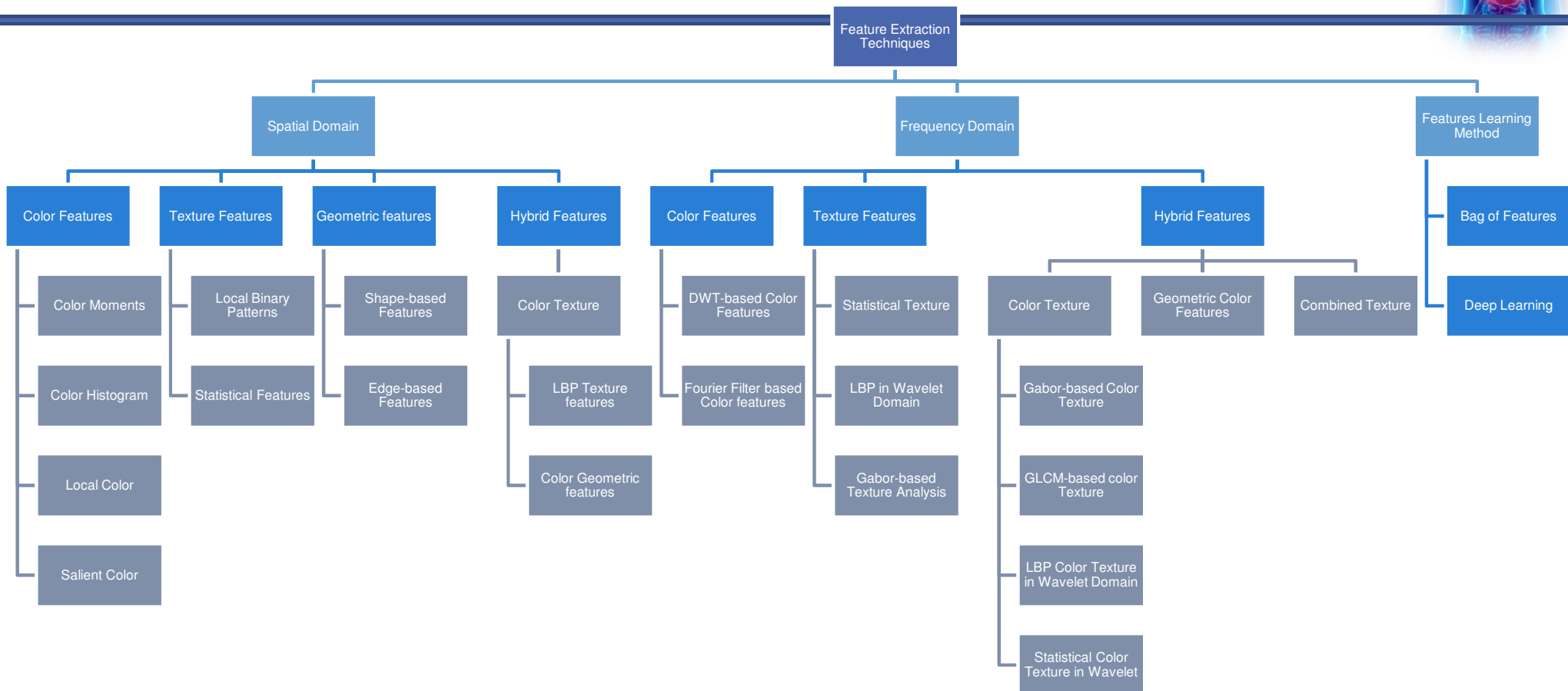
Outline



1. **Introduction**
2. **Literature Review**
3. **Challenges**
4. **Problem Statement**
5. **Proposed Methods**
6. **Results and Discussions**
7. **Conclusion and Future Work**
8. **Contributions**
9. **References**
10. **Questions Answers**



Literature Review

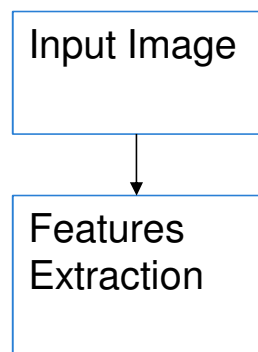


Literature Review (*continued*)



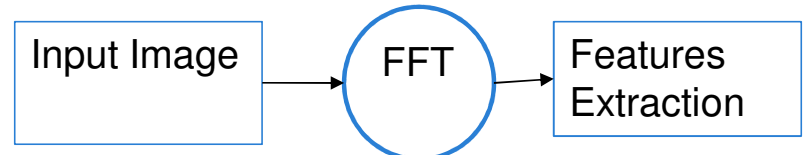
■ Spatial domain

- Features are extracted from pixels of images in spatial domain.

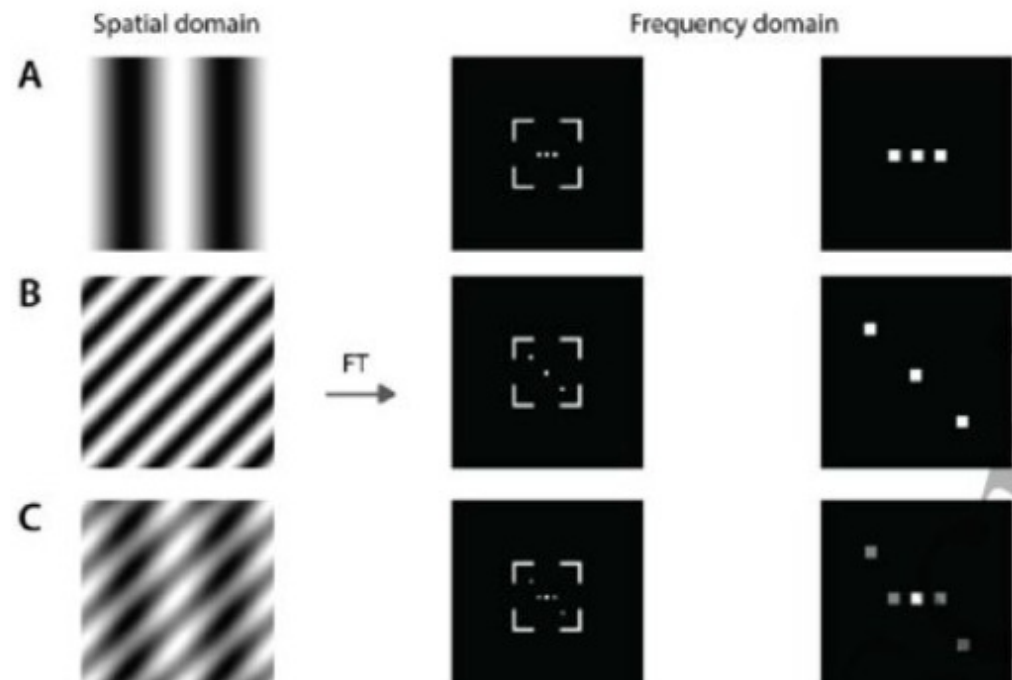


■ Frequency domain

- In Frequency domain, Fourier transform of images is calculated for features extraction

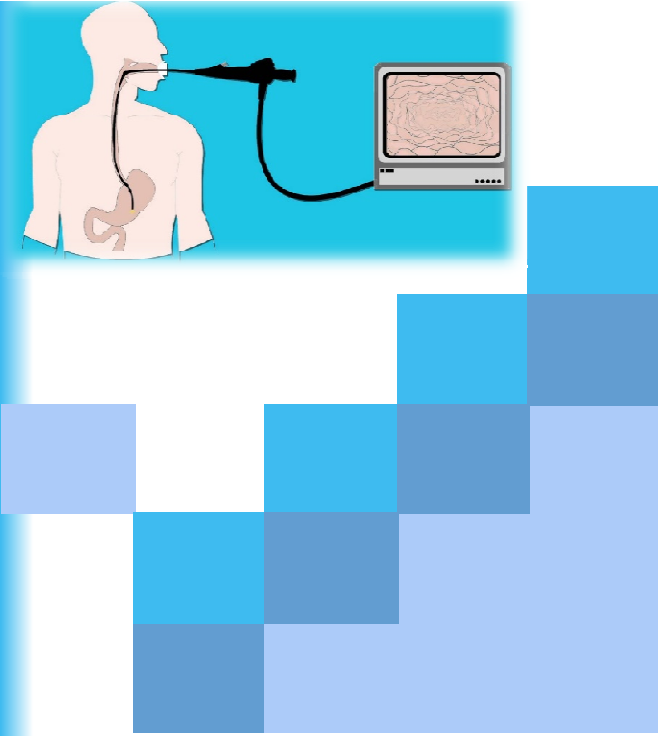


Literature Review (*continued*)



Literature Review (*continued*)

- Several methods have been developed for detection of gastric abnormalities from endoscopic frames.
- Grouped them on the basis of their features, such as Color, Texture and Geometric features.
- Colors: Intensities perceived by human eye.
- Textures: Characteristics of image surface.
- Geometric: Shape based or geometric properties.
- Hybrid Features: Two or more features are combined.
- Feature Learning: BoF and Deep Learning Methods in which features are learned from input data.



Computer-aided Analysis of Endoscopic-frames for the Detection of Abnormalities in
Gastrointestinal Tract

Literature Review (*continued*)

Color Features Extraction Methods In Spatial Domain

Table 2.1: A Summary of Color Features Extraction Methods In Spatial Domain For Computer Aided Diagnosis of Abnormalities in GI-Tract

Ref.	Year	Methods	Results
[1]	2019	An enhancement of computer aided approach for colon cancer detection in WCE Images using ROI based color histogram features and SVM classifier.	95.7% ACC
[2]	2019	HSV and RGB color features are used for the classification of bleeding WCE frames by training SVM classifier.	90.92% ACC
[3]	2019	Colors are computed from color moments and texture results are compared with colors. SVM classifier is used for the classification of frames.	97.7%ACC
[4]	2018	HSV and RGB features for the classification of bleeding WCE frames of GI tract with k-NN classifier and cross validation with k= 5 is used.	99.6% ACC
[5]	2018	Color histogram features for the classification of bleeding frames by training k-NN classifier using cross validation on 1000 WCE images of GI Tract.	96.10%ACC 96.4%SEN 96.01%SPEC
[6]	2016	Statistical moments for the classification of cancer frames by training SVM, NN, and k-NN using LOO-CV on 102 VE images of colon.	77%ACC 91%SEN 62%SPEC
[7]	2015	A and B histogram moments for the classification of bleeding regions, Crohn's disease, suspected tumors, ulcers, polyps by training SVM + MLP using cross validation 10 on 3200 WCE frames of GI tract.	98.0%ACC 97.4%SEN 98.4%SPEC
[8]	2015	Salient color features for the classification of bleeding frames and other anomalies by training SVM with holdout on 800 WCE images of GI tract.	95.89%ACC 98.77%SEN 93.45%SPEC
[9]	2015	Color based CIELAB and selected first-order statistical features from various color components using SVM and saliency for classification of bleeding and other anomalies using SVM cross-validation 10 on 252 cases of WCE of GI tract	96%SEN 91%SPEC 94%ACC

Literature Review (*continued*)

Texture Features Extraction Methods In Spatial Domain

Table 2.2: A Summary of Texture Features Extraction Methods In Spatial Domain For Computer-Aided Diagnosis of Abnormalities in GI-Tract

Ref.	Year	Methods	Results
[10]	2019	GLCM texture features are used for the classification of polyps, ulcer and inflammatory from multiple endoscopy data sets WCE frames.	99.2% SEN
[11]	2019	LBP texture features are used for the classification of ulcer WCE frames.	99.25%ACC 98.51%SEN
[12]	2018	A multi scale frequency and difference based representation (CDR) of image textures for classification is proposed. The local counting vector (LCV) is used to extract different types of textural formations.	99.1% SEN
[13]	2015	Difference based LBP features are used for the classification of ulcer in 207 VE images of colon by training and using 10 cross validation.	90%ACC
[14]	2015	LBP features used for the classification of ulcer from 344 WCE images of small bowel by training SVM by using holdout.	93.16%ACC
[15]	2013	LBP features used for the classification of cancer VE (NBIME) frames such that 57 images are used of which 27 images are of abnormal lesions and 30 normal images of GI tract by unsupervised learning.	100%PRE 87%SEN
[16]	2011	Multi scale local binary pattern (MS-LBP) for the classification of cancer frames, 1200 WCE frames of 10 patients of small bowel are used for training SVM, KNN and ensemble classifiers by using 4 cross validation.	90.50%ACC, 92.33%SEN 88.67%SPEC

Literature Review (*continued*)

Geometric Features Extraction In Spatial Domain

Table 2.3: A Summary of Geometric Features Extraction Methods In Spatial Domain
For Computer Aided Diagnosis of Abnormalities In GI-Tract

Ref.	Year	Methods	Results
[17]	2020	HOG features are used to detect polyps from WCE frames. Then, the polyps are classified using SVM and RUSBoost.	86.33% SEN
[18]	2019	A group of shape probability functions and response intensity functions produced by Hessian matrix eigen values are used to construct RSS filters to enhance boundary areas of bubbles. Then, bubble like frames can be distinguished.	91%SEN
[19]	2016	Edge based features for the classification of Celiac disease in CLE 67 images (class distribution: 31 normal images, 17 with VA and 19 with CH) frames of small bowel by training a linear NB and quadratic NB and using 10 cross validation.	94.03%ACC
[20]	2015	Farctal dimensions for the classification of polyps in NBI 359 images of type A ,462 images of type B and 87 images of type C of colon by training k-NN while using LOO-CV.	88.2%ACC
[21]	2015	Higher Order Local auto correlation (HLAC) for retrieval of multiple types of frames in which 100 VE colon images are used.	-

Literature Review (*continued*)

Hybrid Color Texture Features Extraction In Spatial Domain

Table 2.4: A Summary of Hybrid Color Texture Features Extraction Methods In Spatial Domain For Computer-Aided Diagnosis of Abnormalities In GI-Tract

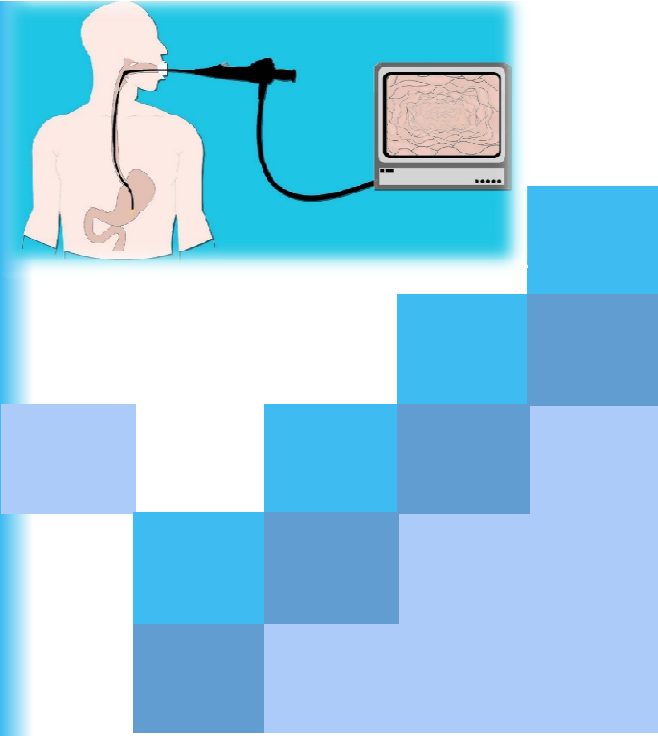
Ref.	Year	Methods	Results
[22]	2019	Color and texture saliency are combined to classify nearly 9000 WCE frames for ulcer and bleeding.	99%ACC
[23]	2018	Statistical moments such as energy, mean, standard deviation, skew, kurtosis, and entropy are computed from histograms of images by representing images in RGB and HIS color spaces on 1200 WCE frames.	91%ACC
[24]	2016	Edge based texture features are calculated from filters and red color for the segmentation of inflammation in VE 3 videos of colon by unsupervised learning.	80%ACC
[25]	2016	Seven histograms (HSV, RGB, LBP) for summary of endoscopy procedure for cancer in VE 2610 frames, 790 over saturated frames, 640 dark frames and 1158 obscure frames (768 x 576) of stomach are used for training random forest (RF) classifier by using holdout 90 ratio 10.	95%ACC
[26]	2015	Color and texture features are used for the classification of cancer frames and 3800 VE images of 1284 patients of small bowel for training SVM by using holdout.	0.9542 AUC
[27]	2015	Color, texture, and edges features are used for the classification of multiple diseases in WCE with 5029 images of GI tract by training HMM and using 3 cross validation.	93.3 %ACC 93.3 %SEN
[28]	2015	LBP features are used for image sequence reduction and summarization. Color moments RGB, color moments HSV and color histogram are used for the classification of multiple types of diseases in WCE. 10671 images (256 x 256) of GI tract are used.	88.3%ACC

Literature Review (*continued*)

Hybrid Geometric Color and Geometric Texture Extraction In Spatial Domain

Table 2.5: A Summary of Hybrid Geometric Color and Geometric Texture Features Extraction Methods In Spatial Domain For Computer Aided Diagnosis of Abnormalities In GI-Tract

Ref.	Year	Methods	Results
[29]	2019	Based on pixel values region growing and region merging, techniques are applied to gastric frames for the segmentation of abnormalities where 10 WCE images are used.	94.05%ACC
[30]	2018	HVLAD is formed to encode local descriptors to obtain a global descriptor. Finally, by fusing an average Spatial Pyramid Pooling, multi scale SDMD is carried out to produce an MSDMD based texture descriptor.	94.03%ACC
[31]	2015	SIFT and CCH are combined for the classification of WCE frames with gastro esophageal reflux disease. 147 images of esophagus are used by training hierarchical heterogeneous descriptor fusion support vector machine (HHDFSVM) and using 10 cross validation.	93.2%ACC, 94.9%SEN and 92.6%SPEC
[32]	2015	Histogram, PHOG and LBP features for the classification of gastritis, cancer, bleeding and ulcer in VE 6000 images of GI tract by unsupervised learning.	74.31%ACC
[33]	2015	Geometric and topological features for the classification of cancer in VE (NBI-ME) 90 frames (786x576) of GI tract for training ensemble method (Adaboost) by using LOOCV.	90%ACC
[34]	2015	HOG+SIFT+LBP + (COLOR + Texture saliency) features are used for the classification of ulcer in WCE. 170 ulcer and 170 normal images of 20 patients of GI tract for training Locality constrained Linear Coding (LLC) by using 5 cross validation.	92.65%ACC 94.12%SEN
[35]	2015	Local features and global texture features used for the classification of cancer in endoscopic ultrasonography of 66 patients with early esophageal cancer (mean age 53 years; age range 21-87 years; 32 male and 34 female total 91 patients (mean age 42 years; age range 32-75 years; 39 male and 52 female) and trained SVM by using 10 crossvalidation	93%ACC 89.4%SEN 94%SPEC



Frequency Domain



Literature Review (*continued*)

Color Features Extraction Methods In Frequency Domain

Table 1.6: A Summary of Color Features Extraction Methods In Frequency Domain For Computer Aided Diagnosis of Abnormalities In GI-Tract

Ref.	Year	Methods	Results
[36]	2015	Fractal Dimensions and DWT used for the classification of cancer in VE. 10 images (1024 x 1024) of esophagus with unsupervised learning.	-
[37]	2010	Dual Tree Complex Wavelet Transform (DTCWT) for retrieval of multiple abnormalities in VE 627 images of colon by training discriminant classifier with LOO-CV.	96%ACC, 94%SEN and 97%SPEC
[38]	2010	Fourier features for classification of cancer in ZE 484 images of 53 patients (624 533) are used of colon for training SVM, discriminant analysis and NB using LOO-CV	96.9%ACC 2 classes and 86.8%ACC 6 classes
[39]	2009	Gaussian MRF and color DWT pyramidal for the classification of cancer of VE (286 neoplastic cases, 198 nonneoplastic cases of colon) by training k-NN and NB while using LOO-CV.	92.8%ACC

Literature Review (*continued*)

Texture Features Extraction Methods In Frequency Domain

Table 1.7: A Summary of Texture Features Extraction Methods In Frequency Domain
For Computer Aided Diagnosis of Abnormalities In GI-Tract

Ref.	Year	Methods	Results
[40]	2018	Gabor and other texture descriptors used for the classification of endomicroscopy frames for Barrett's esophagus.	90.0% AUC
[41]	2015	DDFT based texture descriptor for the classification of WCE bleeding frames. 32 videos of 600 bleeding and 600 non-bleeding frames of 12 patients are used, test set consists of 860 bleeding and 860 non-bleeding frames by training SVM classifier and using holdout method.	99.19%ACC 99.41%SEN 98.95%SPEC
[42]	2015	Contour let transform and LoG filter used for the classification of ulcer in WCE frames, 137 images are used of which 65 are ulcer and 72 are normal of GI tract by training SVM and using 10 cross validation.	94.16%ACC
[43]	2012	Gabor texture autocorrelation for shift invariance of SGFS by using invariance properties of Gabor filters and text on framework: Texton AGF for the classification of cancer in chromoendoscopy (CH) and narrow band imaging (NBI) with 142 CH and 224 NBI images are used. SVM is trained using 10 cross validation.	83%ACC 82%SEN 82%SPEC 0.85 AUC
[44]	2011	Gabor textures for the classification of cancer in CH and NBI, 176 CH images and 221 NBI of GI tract are used by training statistical classifier with 10 cross validation.	83.9%ACC
[45]	2009	Texture features curve let transform LBP for the classification of ulcer in WCE 100 images (256x256) of small bowel by training SVM and ANN while using cross validation.	93.28%ACC, 92.37%SPEC 91.46%SEN
[46]	2009	DT-CWT+Gabor Wavelet texture for the classification of cancer in ZE 484 images of GI Tract by training k-NN and using LOO-CV.	93.39%ACC

Literature Review (*continued*)

Hybrid Color Texture Features Extraction Methods In Frequency Domain

Table 1.8: A Summary of Hybrid Color Texture Features Extraction Methods In Frequency Domain For Computer Aided Diagnosis of Abnormalities In GI-Tract

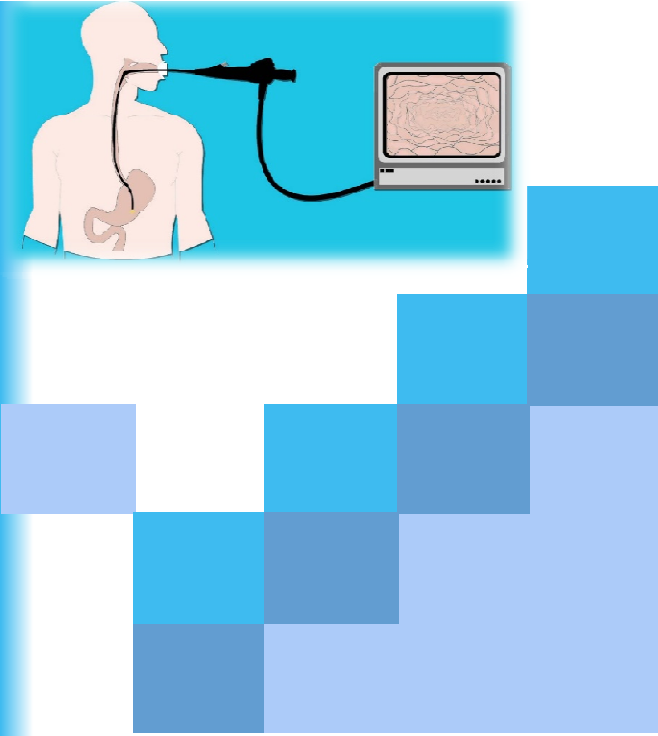
Ref.	Year	Methods	Results
[47]	2019	Color Features HSV and RGB are combined with wavelets for the classification of CLE images.	99.12%acc
[48]	2016	Local Gabor and color features for the classification of cancer in HDVE 100 images of 39 patient dataset of esophagus by training RF classifier and using LOO-CV.	90%SEN
[49]	2016	Fourier descriptors, HIS, and statistical features for the classification of cancer in VE. 280 images of 26 real cases of patients (10 healthy and 16 suffering from the disease) of esophagus by training k-NN criterion and RF classifier while using holdout.	86%SEN 72%SPEC
[50]	2015	LBP with CIE XYZ color features for the classification of bleeding in 332 WCE images comprising of 145 bleeding images and 187 normal images of GI tract by training kNN and using 10 cross validation.	0.9638 AUC
[51]	2014	Local color and Gabor texture based features for the classification of cancer in ZE 32 images of esophagus by training SVM while using LOO-CV.	95%SEN 75%pre

Literature Review (*continued*)

Hybrid Geometric Color, and Texture Extraction Methods In Frequency Domain

Table 1.9: A Summary of Hybrid Geometric Color, and Texture Features Extraction Methods In Frequency Domain For Computer Aided Diagnosis of Abnormalities In GI-Tract

Ref.	Year	Methods	Results
[52]	2019	Color and texture features are combined for the classification of cancer using multiple classifiers trained on 176 images with 10 cross validation.	87.2% ACC
[53]	2018	Gabor texture and GLCM texture features are combined for the classification of cancer frames by using multiple classifiers and 176 images are used via 10 cross validation.	87.2% ACC
[54]	2014	Leung' Malik and LBP texture features are used for the classification of ulcer, bleeding, and polyps from WCE. 800 images of colon are used for training kNN by using 10 cross validation.	91%SEN 90.8% SPEC
[55]	2010	Gabor texture, k-mean and geometric features for the classification of polyps in WCE. 128 images, 64 images with polyps and 64 normal of colon are used by unsupervised methods.	100%SEN 81%SPEC
[56]	2009	SUSAN Edge detector and LoG used for the classification of polyps in 50 frames WCE videos containing 10 frames with polyps and 40 normal frames of small bowel by training fuzzy-SVM and using holdout.	100%SEN and 67.5%SPEC



Feature Learning Methods

Computer-aided Analysis of Endoscopic-frames for the Detection of Abnormalities in
Gastrointestinal Tract

Features Learning Methods

- **Bag of Features:** where dictionary of features is learned. These can be colors or textures.
- **Features Learning:** Convolutional Neural Network is used for learning features from input data



Literature Review (*continued*)

Bag of Features

Table 1.10: Bag of Features Methods for classification of Gastric Images

Ref.	Year	Methods	Results
[57]	2017	Color CIELUV adapted histogram with BOF model for the classification of cancer is used, 130 CH images of GI tract used by training k-NN, NB, SVM, and DT while using 10 cross validation.	88%SEN and 0.93AUC
[58]	2016	Colors with BOF model for the classification of multiple abnormalities in VE, 12000 images of 424 people of esophagus used for training online metric learning by using 10 cross validation. 10	0.93AUC
[59]	2015	SIFT with BOF model for the classification of cancer in NBI 587 cutout images of gastric cancer and 503 cutout images of surrounding tissue of GI tract by training SVM and using holdout.	86.5%ACC
[60]	2015	Color with BOF Model YCbCr histogram for the classification of bleeding in 2400 WCE images that consist of 400 bleeding frames and 2000 normal frames (256 x256) of GI tract by training k-NN and SVM while using 10 cross validation.	95.75%ACC, 92%SEN, 96.5%SPEC and 0.97AUC
[61]	2015	SIFT with BOF Model for the classification of multiple abnormalities in WCE images (450 normal, 450 abnormal and second dataset with 600 normal, 600 abnormal of WCE images of colon by training SVM and using holdout.	98.25%ACC
[62]	2010	Dense SIFT with BOF models are used for retrieval in CLE 1036 images of GI Tract by training k-NN while using LOO-CV.	89%ACC

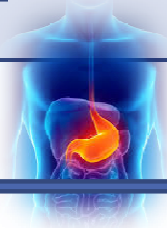
Literature Review (*continued*)

Deep Learning Methods

Table 1.11: Features Learning Methods For Computer-aided diagnoses of Abnormalities in GI Tract

Ref.	Year	Method	Results
[63]	2018	CNN is used for the classification of cancer in VE of GI tract. ANN is trained on 13000 images using holdout.	98%ACC 92%SEN
[64]	2018	CNN is used for the classification of hookworms by training ANN on 440000 WCE images of GI tract by using holdout.	88.5% ACC
[65]	2017	CNN is used for the classification of polyp frames in colon by training SVM on 1970 VE 332 NBI images by using 3 cross validation.	99.4% ACC
[66]	2017	CNN is used for the detection of polyps in colon by training ANN on 3257 images by using holdout.	94.0% ACC
[67]	2017	CLE frames of GI tract and patch based CNN are trained for the segmentation of cancer detection and ensemble classifier is trained using 1400 images by holdout.	91.09% ACC
[68]	2015	WCE frames of GI tract are used to train CNN for the classification of multiple diseases using NELM such that 60000 images are used for training and 15000 images for testing (480x480) by using holdout.	97.25%ACC
[69]	2015	CNN is used for providing summary of multiple DCNN of 25 cases (60000 training images and 15000 testing images using holdout).	95%ACC
[70]	2011	Color features are used for the classification of bleeding frames. 50000 WCE frames of GI tract are used for training PNN by using holdout method.	93.1%SEN 85.6%SPEC

Literature Review (*continued*)



Insights

- Most of the existing methods tested on private datasets.
- Gastric lesion do not have any specific geometric structure.
- Much work is done for hybrid color-texture feature extraction approaches.
- Existing feature extraction methods are for general recognition applications.
- Inefficiently cope with dynamics of gastric environment.
- Less work on chromoendoscopy images.



Outline

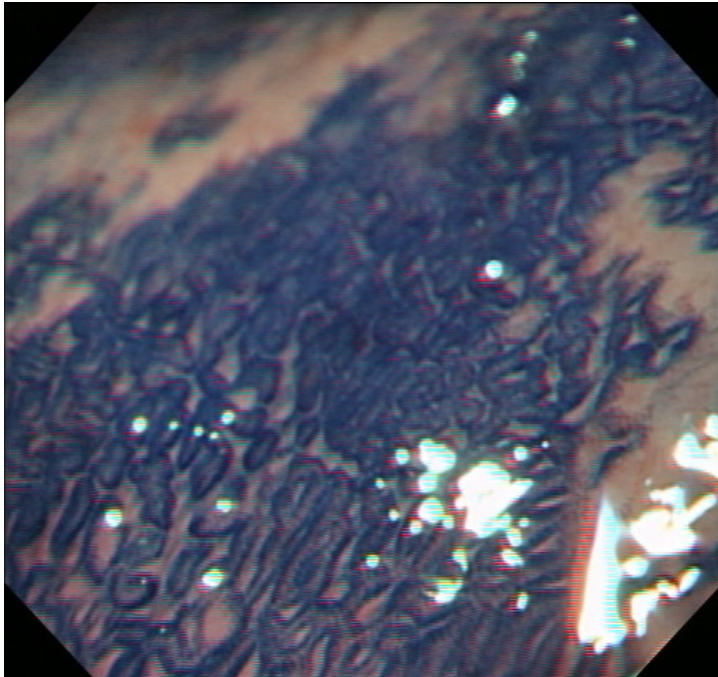
1. Introduction
2. Literature Review
3. Challenges
4. Problem Statement
5. Proposed Methods
6. Results and Discussions
7. Conclusion and Future Work
8. Contributions
9. References
10. Questions Answers



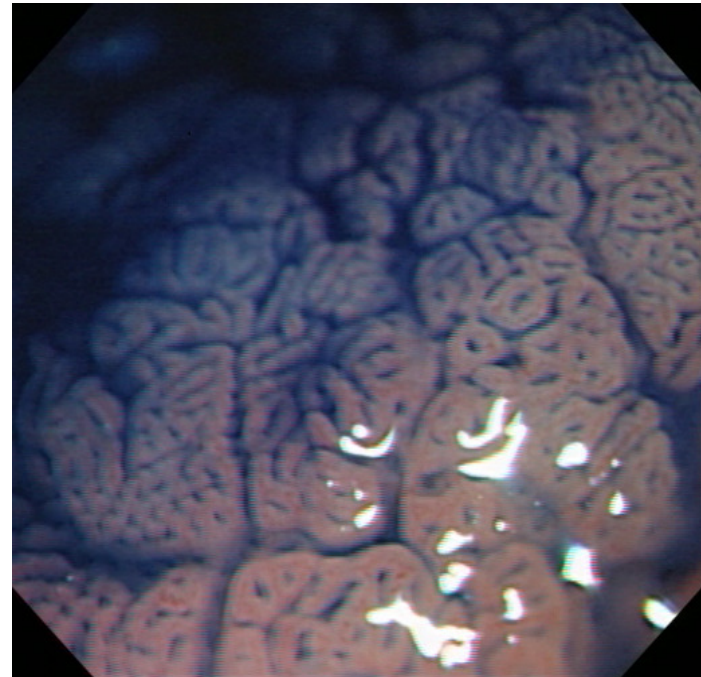
Challenges



Abnormal frame



Normal frame



Difference in texture

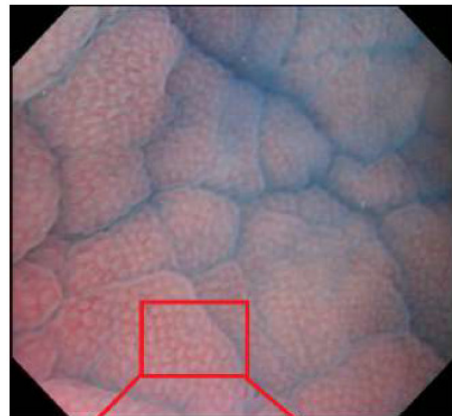
Computer-aided Analysis of Endoscopic-frames for the
Detection of Abnormalities in Gastrointestinal Tract



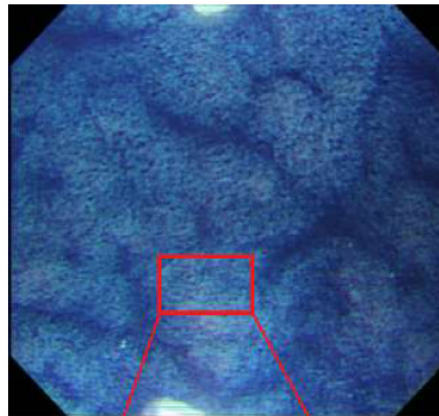
Challenges



Normal frame



Abnormal frame



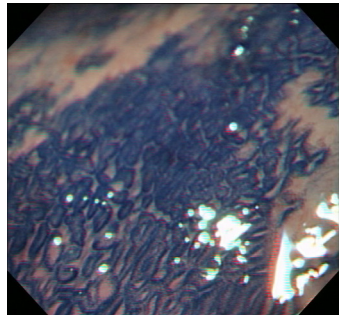
(a)



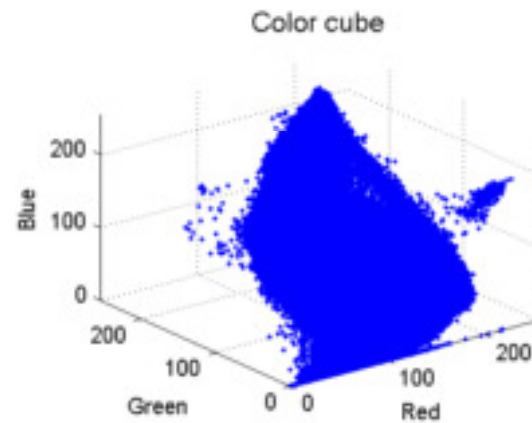
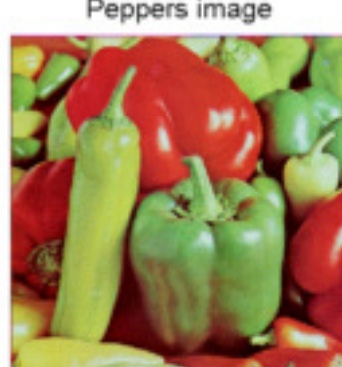
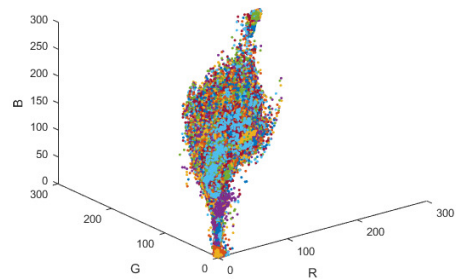
(b)



Challenges



Lack of sufficient color space



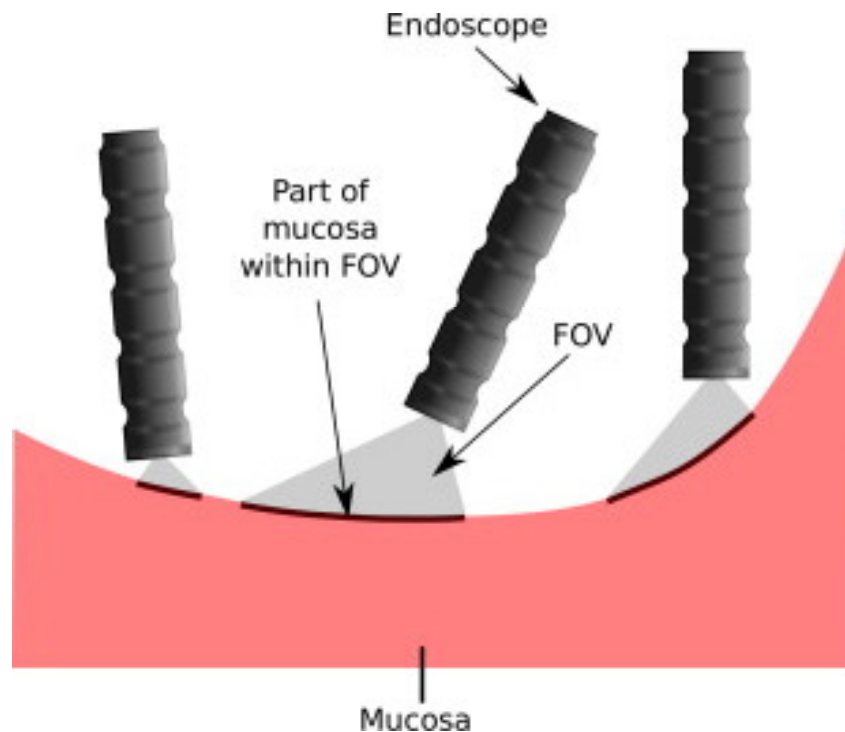
Computer-aided Analysis of Endoscopic-frames for the
Detection of Abnormalities in Gastrointestinal Tract





Challenges

Scale, Rotation, Translation invariance



Outline



1. Introduction
2. Literature Review
3. Challenges
4. Problem Statement
5. Proposed Methods
6. Results and Discussions
7. Conclusion and Future Work
8. Contributions
9. References
10. Questions Answers



Problem Statement



- Existing systems lack in achieving high accuracy due to **dynamics of GI environment**, the endoscopic images suffering from a different group of symmetries (**e.g. translation, rotation, illumination, and scale**) may also have instrument inclusion, poor cleansing, light reflections and presence of air bubbles. There is a need to design **more robust descriptors** which could reflect main characteristics of abnormal regions.



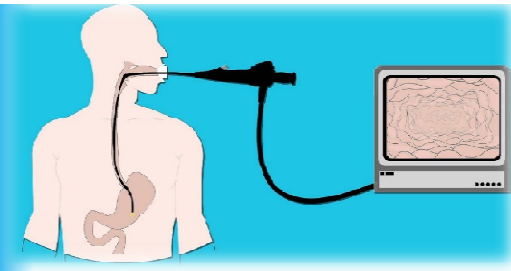
Outline

1. Introduction
2. Literature Review
3. Challenges
4. Problem Statement
5. **Proposed Methods**
6. Results and Discussions
7. Conclusion and Future Work
8. Contributions
9. References
10. Questions Answers



Proposed Methods

1. Classification of chromoendoscopy images using homogeneous texture descriptors (**GHT**).
2. Gastric abnormalities detection using hybrid texture descriptors for chromoendoscopy images (**G2LCM**).
3. **DeepGLCM** and **LGLCM** Texture Features for Classification of Gastric Abnormalities.
4. Framework for Automatic Segmentation of Gastric Images.
5. Deep Learning Features.



Method 1

Classification of chromoendoscopy images using homogeneous texture descriptors.

■ Method 1

Gabor Filter



A 2D Gabor function $g(x, y)$ with spatial coordinates x and y is defined in Eq. 3.2.1. Let $G(u, v)$ be the Fourier transform of $g(x, y)$ as a function of frequency components u and v that are described in Eq. 3.2.2.

$$g(x, y, \sigma, \Omega) = \left(\frac{1}{2\pi\sigma_x\sigma_y} \right) \exp \left[-\frac{1}{2} \left\{ \frac{x^2}{\sigma_x^2} + \frac{y^2}{\sigma_y^2} \right\} + 2\pi j\Omega x \right] \quad (3.2.1)$$



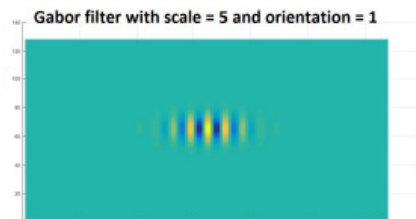
Method 1

Gabor Filter

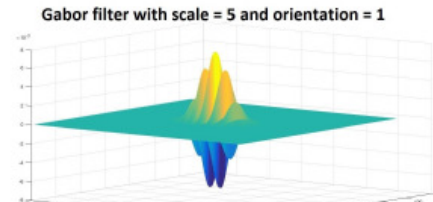


$$G(u, v, \sigma, \Omega) = \exp \left\{ -\frac{1}{2} \left(\frac{(u-\Omega)^2}{\sigma_u^2} + \frac{v^2}{\sigma_v^2} \right) \right\} \quad (3.2.2)$$

where, $\sigma_u = \frac{1}{2\pi\sigma_x}$, $\sigma_v = \frac{1}{2\pi\sigma_y}$



(a)



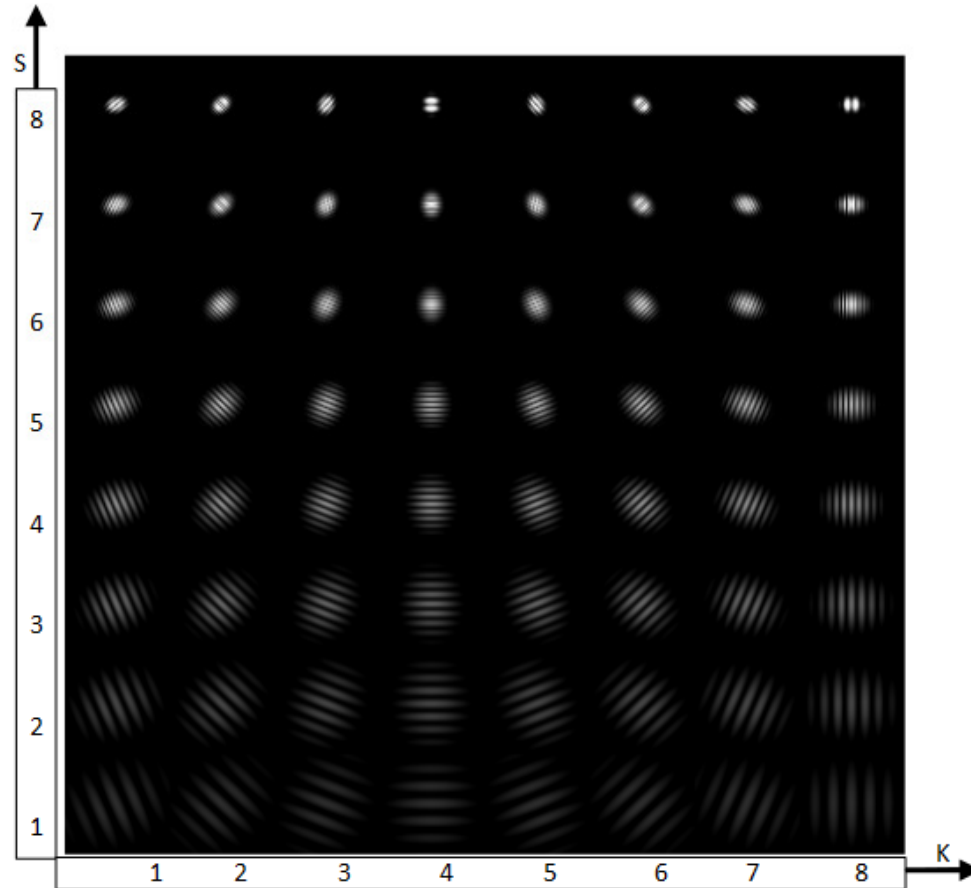
(b)

Figure 3.3: (a) 2D view of spatial kernel of Gabor filter with orientation = 0 and scale = 5 and (b) 3D view of spatial kernel of Gabor filter with orientation = 0 and scale = 5.

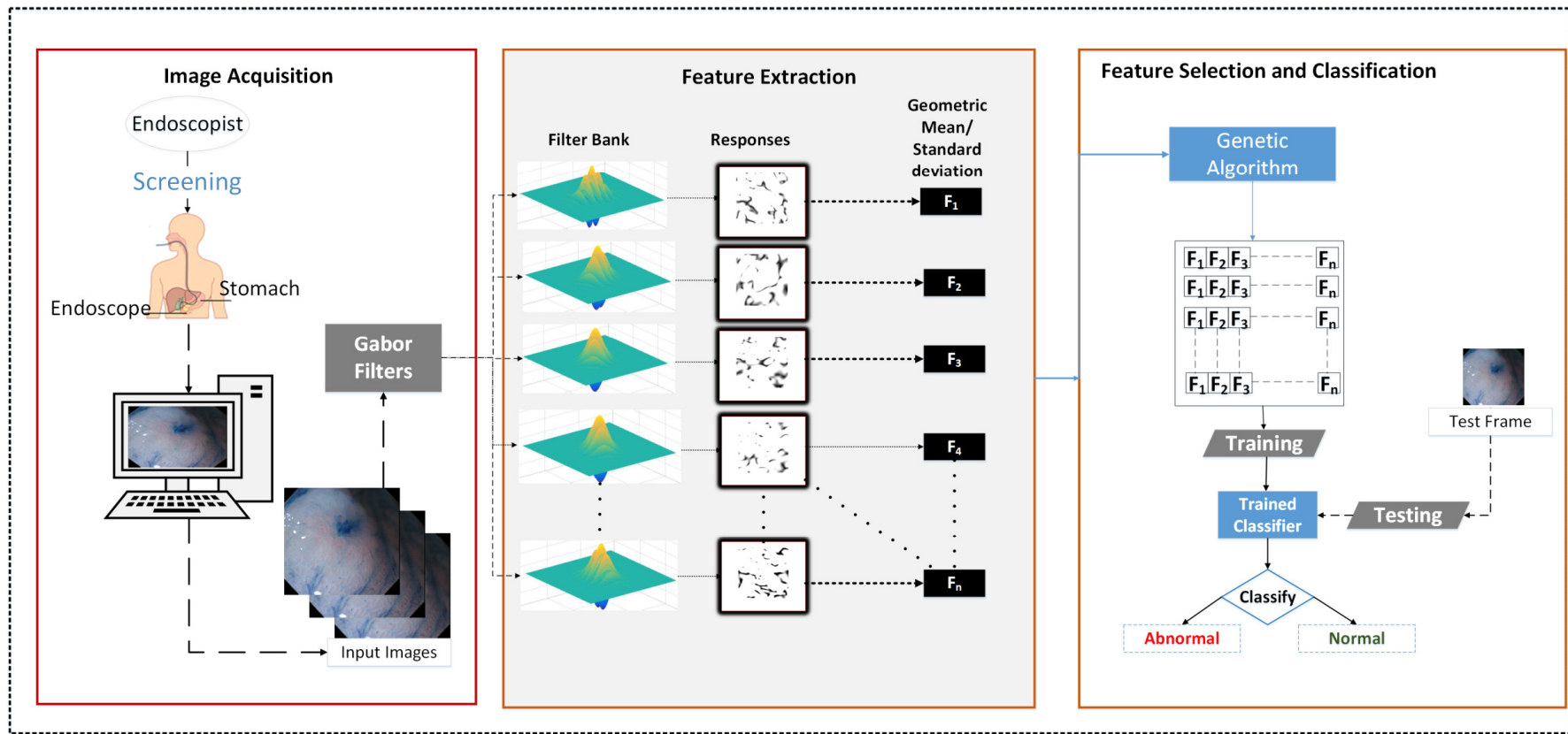


Method 1

Filter Bank

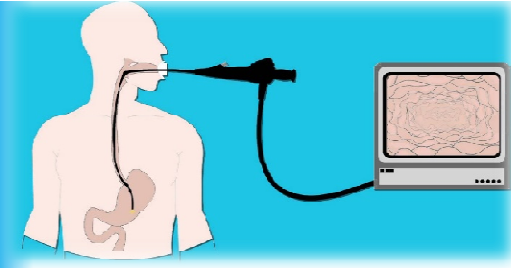


Method 1



Computer-aided Analysis of Endoscopic-frames for the
Detection of Abnormalities in Gastrointestinal Tract

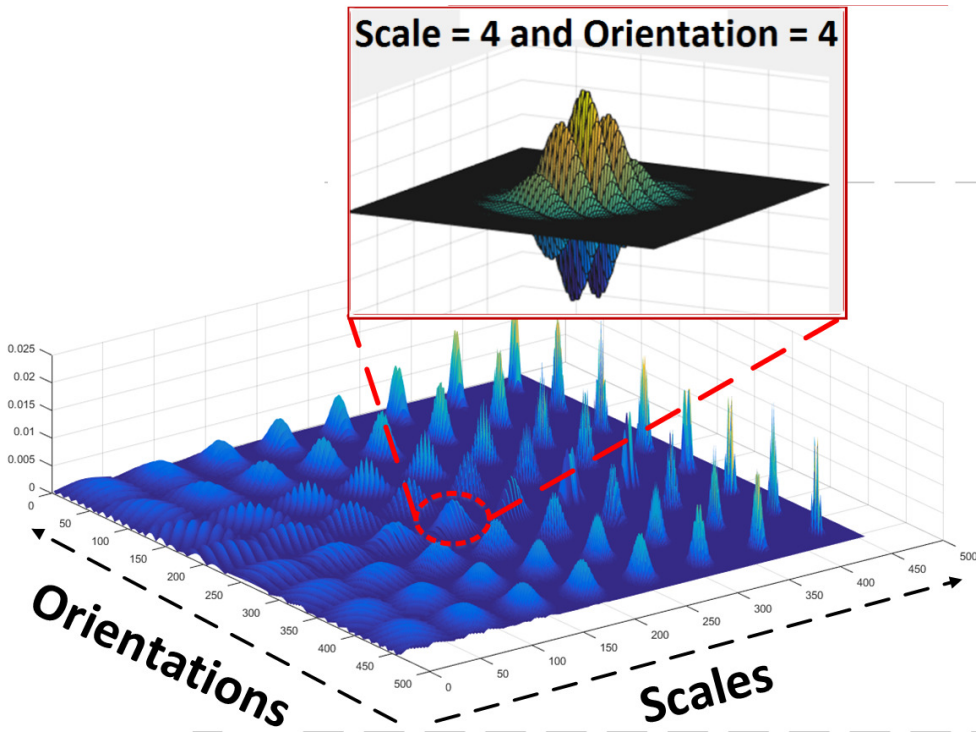




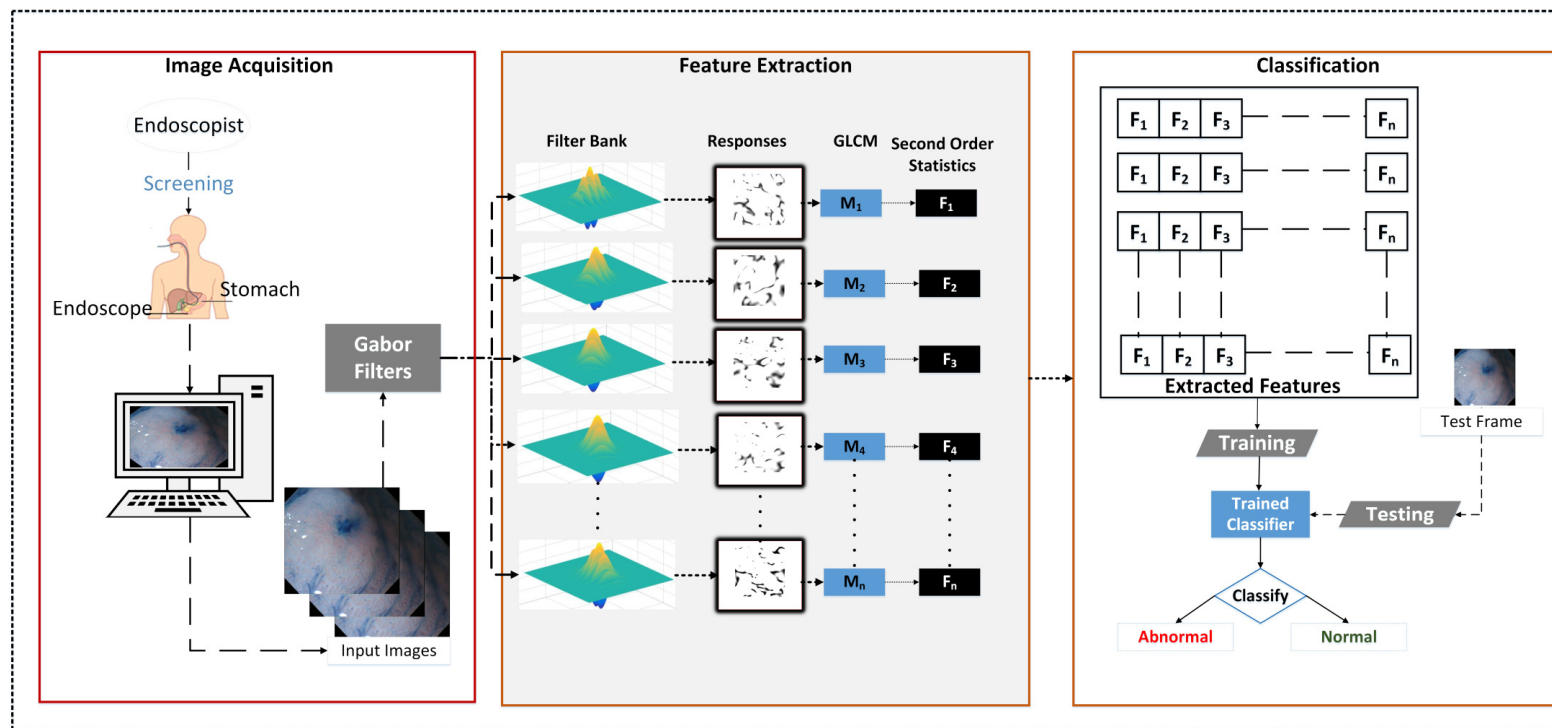
Method 2

Gastric abnormalities detection using hybrid texture descriptors for chromoendoscopy images (G2LCM)

Method 2

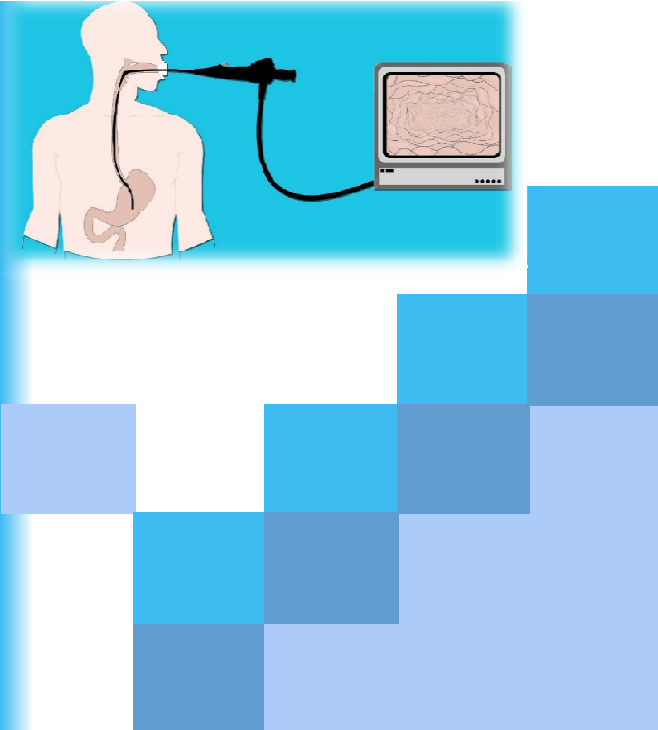


Method 2



Computer-aided Analysis of Endoscopic-frames for the
Detection of Abnormalities in Gastrointestinal Tract

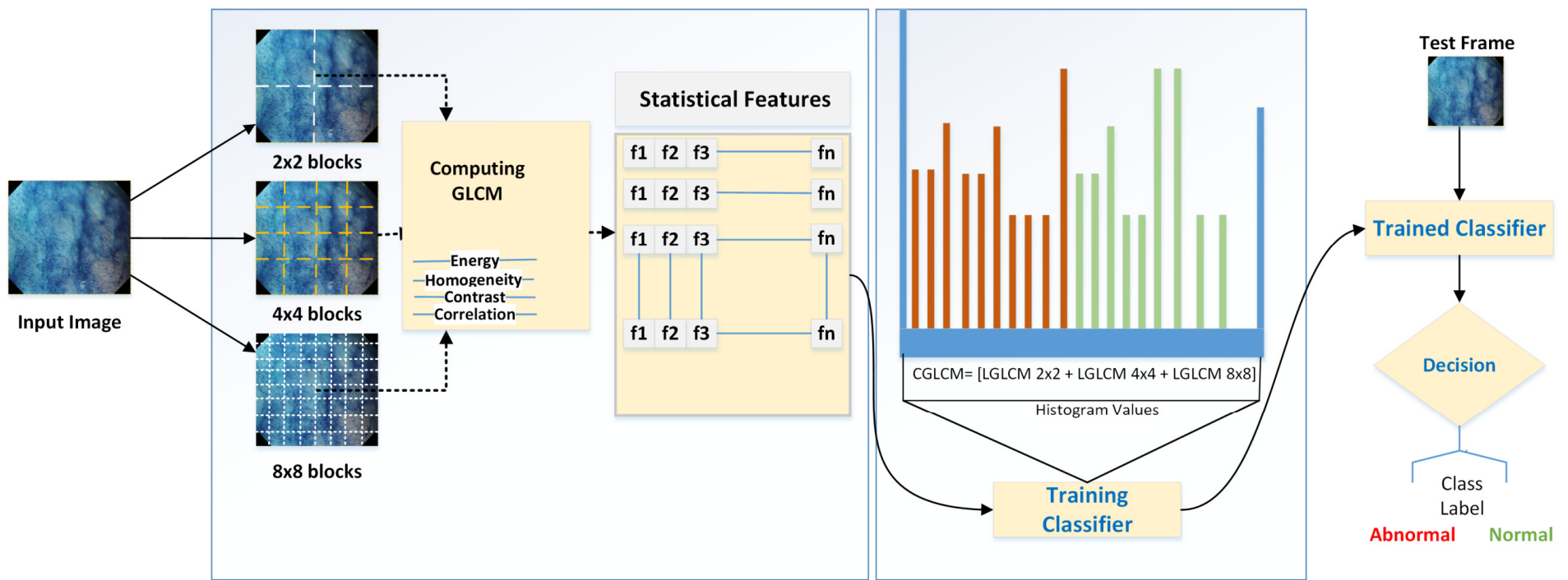




Method 3

DeepGLCM and LGLCM Texture Features for Classification of Gastric Abnormalities

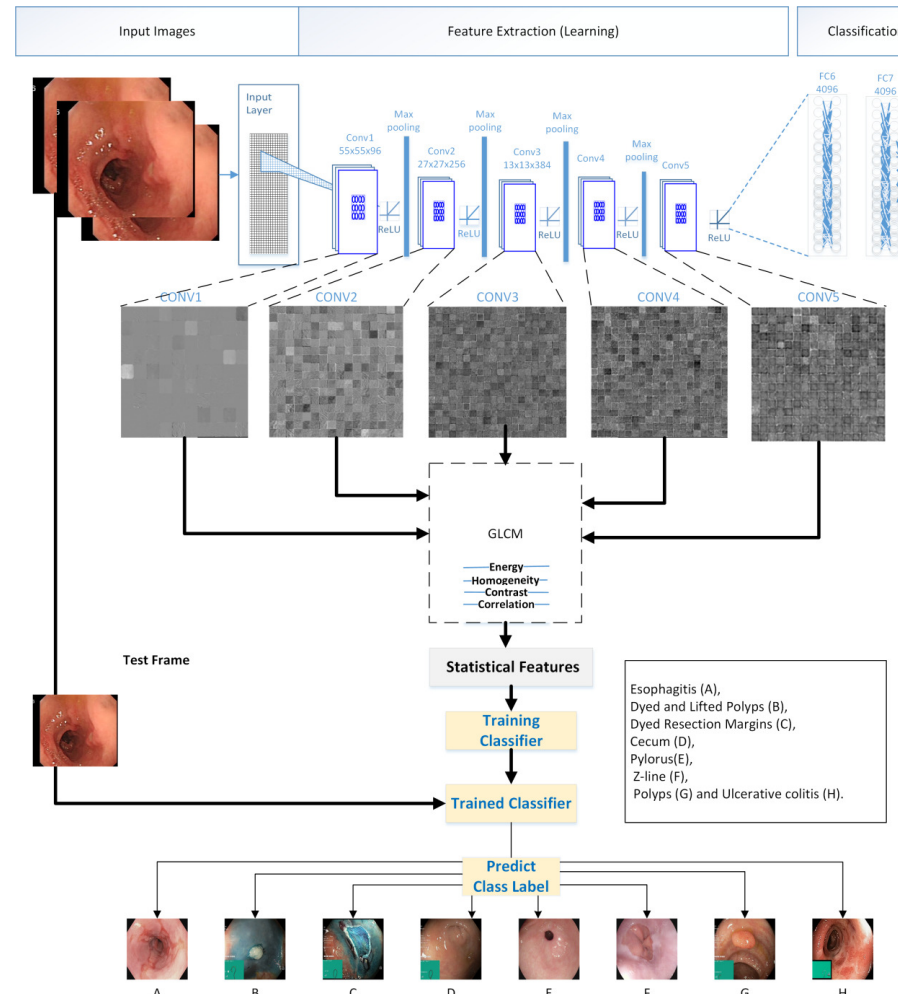
Method 3



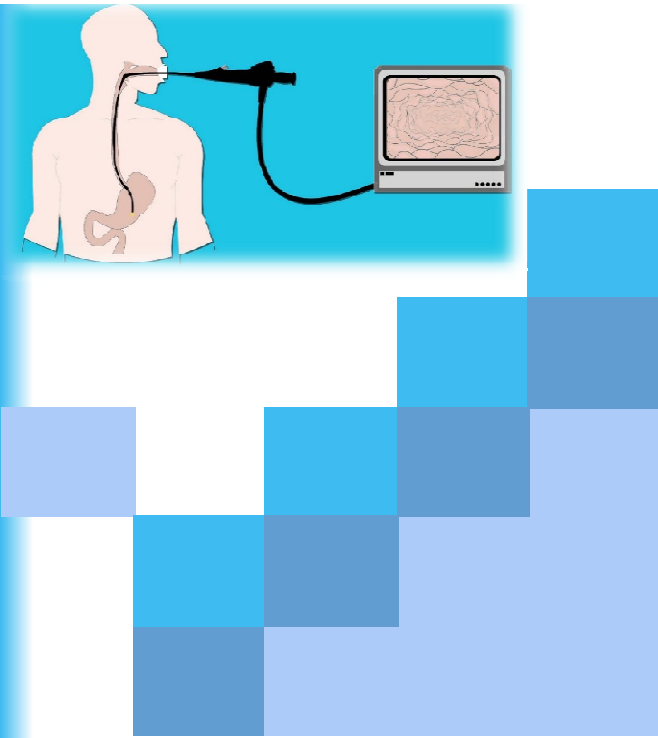
Computer-aided Analysis of Endoscopic-frames for the
Detection of Abnormalities in Gastrointestinal Tract



Method 3



Computer-aided Analysis of Endoscopic-frames for the
Detection of Abnormalities in Gastrointestinal Tract

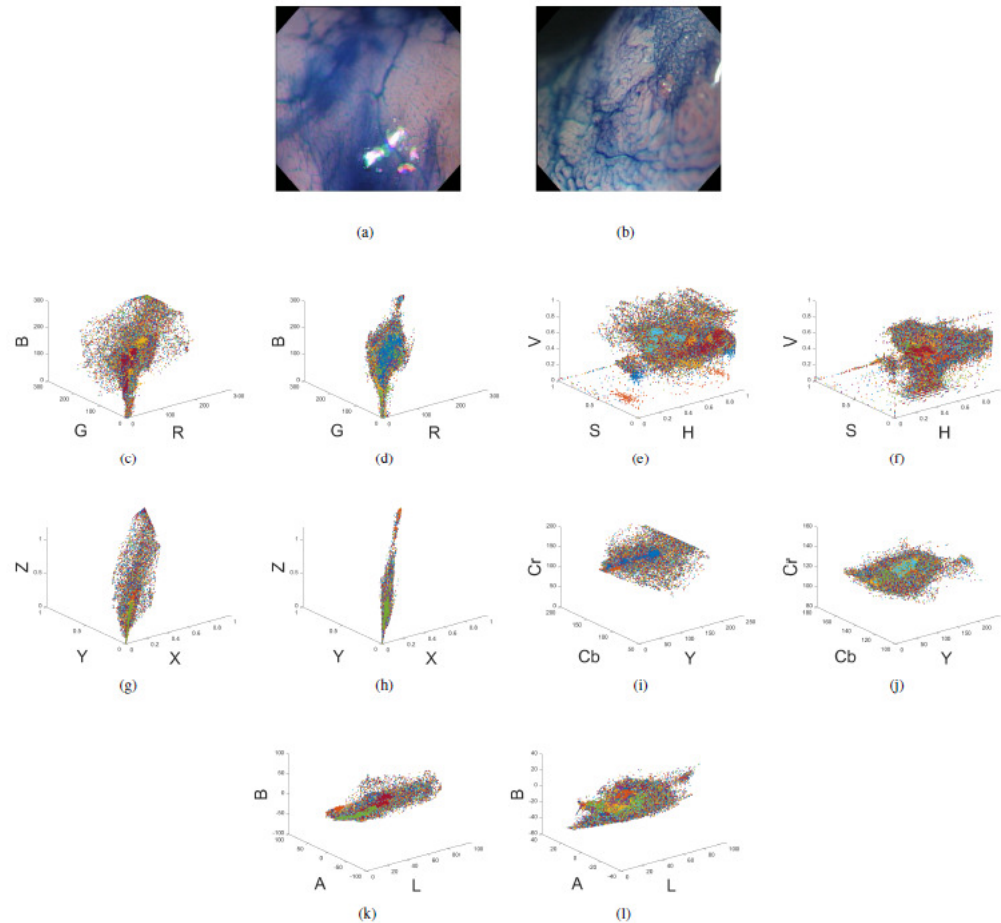


Method 4

Framework for Automatic Segmentation of Gastric Images

Computer-aided Analysis of Endoscopic-frames for the Detection of Abnormalities in
Gastrointestinal Tract

Method 4



Computer-aided Analysis of Endoscopic-frames for the
Detection of Abnormalities in Gastrointestinal Tract



■ Method 4



Algorithm 1 Steps Involved in Image-level and Lesion-level Classification of CH images

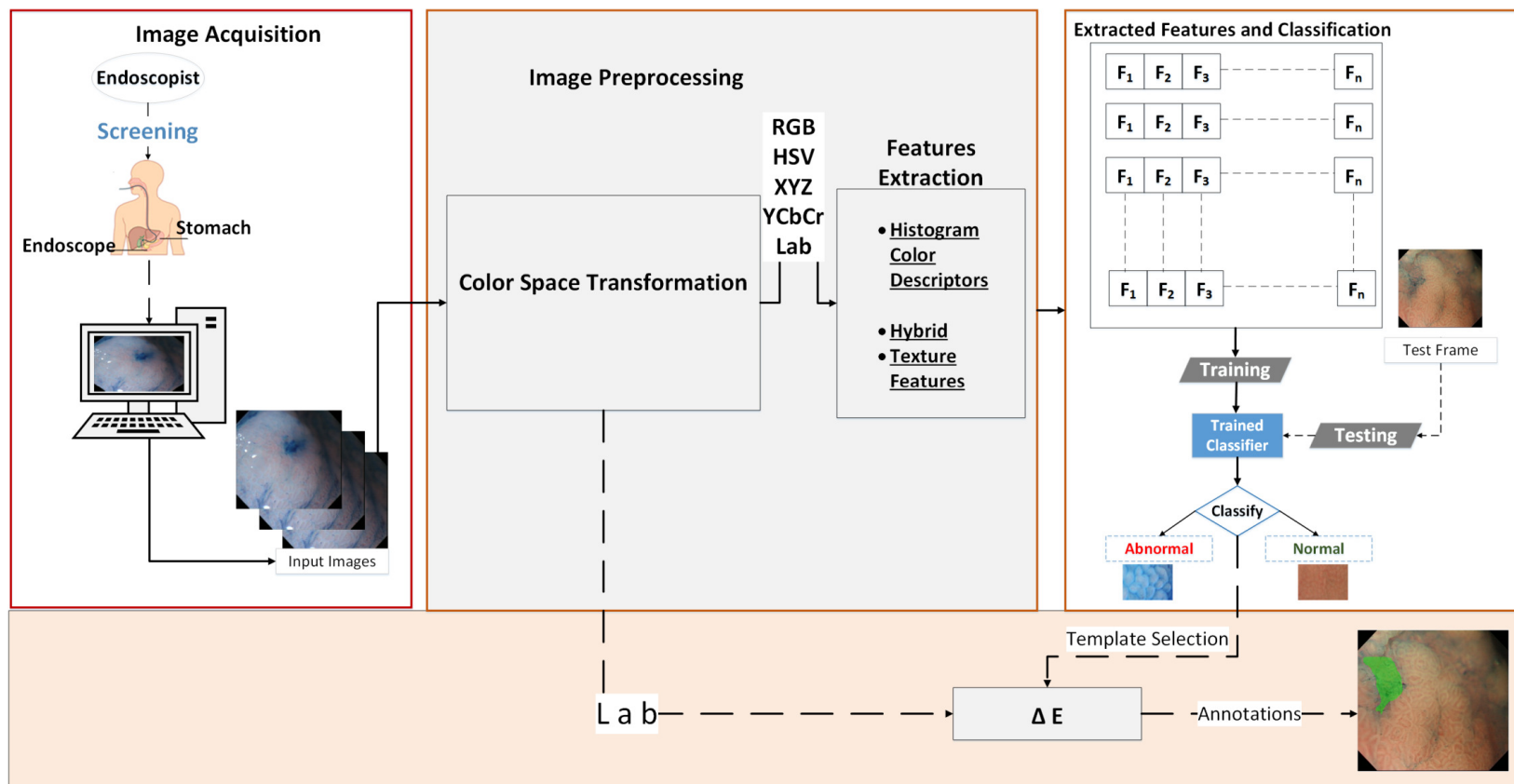
Input: *CH Frames* in

Output: *Decision* out

- 1: Color Space Transformation // *convert images into different color spaces*
 - 2: **if** Lesion-level Classification **then**
 - 3: Apply ΔE for Selection of ROI // *for lesion-level classification*
 - 4: Extract Histogram Features From Lesions
 - 5: **else**
 - 6: Extract Histogram Features from Whole CH Images // *for image-level classification*
 - 7: **end if**
 - 8: Split Data-set Using Cross Validation // *randomly select data for training and testing*
 - 9: Train SVM Classifier By Providing Class Labels \in (Abnormal, Normal)
 - 10: The Trained Classifier Tested with Test-set
 - 11: **return** Class-labels of the Test-set
-

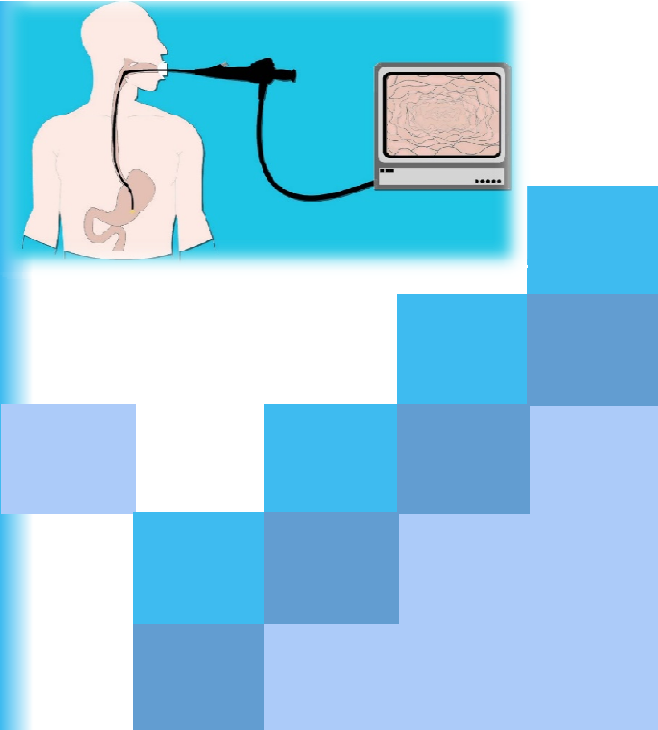


Method 4



Computer-aided Analysis of Endoscopic-frames for the
Detection of Abnormalities in Gastrointestinal Tract



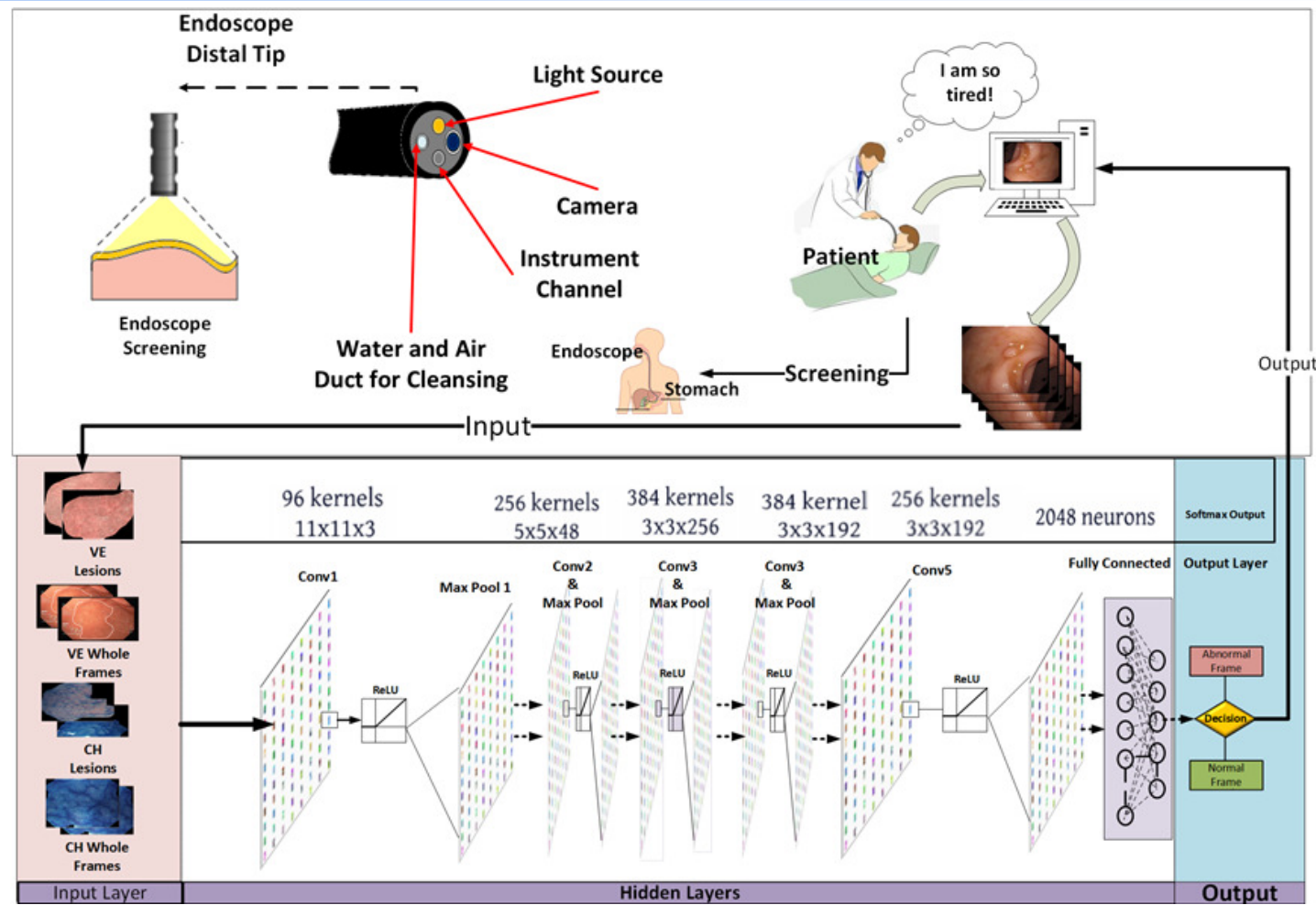


Method 5

Classification of endoscopy images using Deep neural network



Method 5



Computer-aided Analysis of Endoscopic-frames for the Detection of Abnormalities in Gastrointestinal Tract

Outline

1. Introduction
2. Literature Review
3. Challenges
4. Problem Statement
5. Proposed Methods
6. **Results and Discussions**
7. Conclusion and Future Work
8. Contributions
9. References
10. Questions Answers



Results and Discussions



Accuracy Measures

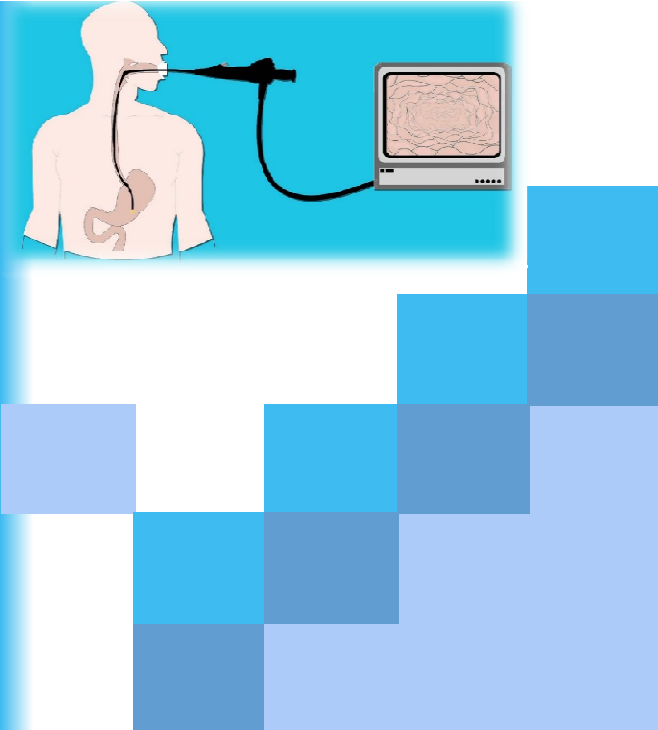
#	Description	Formula
1	True Negative (TN), False Negative (FN), False Positive (FP) and True Positive (TP).	
2	Accuracy	$\frac{TP + TN}{(TP + TN + FP + FN)}$
3	Area under the curve	$\int_{-\infty}^{+\infty} TPR(t)FPR'(t) dt$
4	Sensitivity or True Positive Rate (TPR)	$\frac{TP}{(TP + FN)}$
5	Specificity or True Negative Rate (TNR)	$\frac{TN}{(TN + FP)}$
6	False Positive Rate (FPR)	$FPR = \frac{FP}{FP + TN} = (1 - SPC)$
7	False Negative Rate (FNR)	$FNR = \frac{FN}{TP + FN} = (1 - TPR)$



Results and Discussions

Available Datasets

Ref	Dataset	No. of Images	Endoscopy	Disease	GI. Area	Description
[71]	Chromogastro	176	CH	Cancer	Stomach	518x481 (*.png)
[72]	Private	160	VE+NBI	Cancer	Stomach	1350x1080 (*.tif)
[73]	CLE_barrett	262	CLE	Barret	Esophagus	1024x1024 (*.jpg)
[74]	CLE_celiachy	181	CLE	Celiac	Esophagus	1024x1024 (*.jpg)
[75]	kvasir-dataset	4000	VE	multiple	Stomach	720 x 576 (*.jpg)



Method 1 Results Classification of chromoendoscopy images using homogeneous texture descriptors

Method 1 Results

Experimental Setup



Experimental Setup	
Parameters	Values
Features	Geometric Features
Classifiers	SVM (linear), NB, DT, LDA, Ensemble
Images	Chromoendoscopy
Validation Method	Crossover 10
Average Over	100 iterations
Optimization	GA

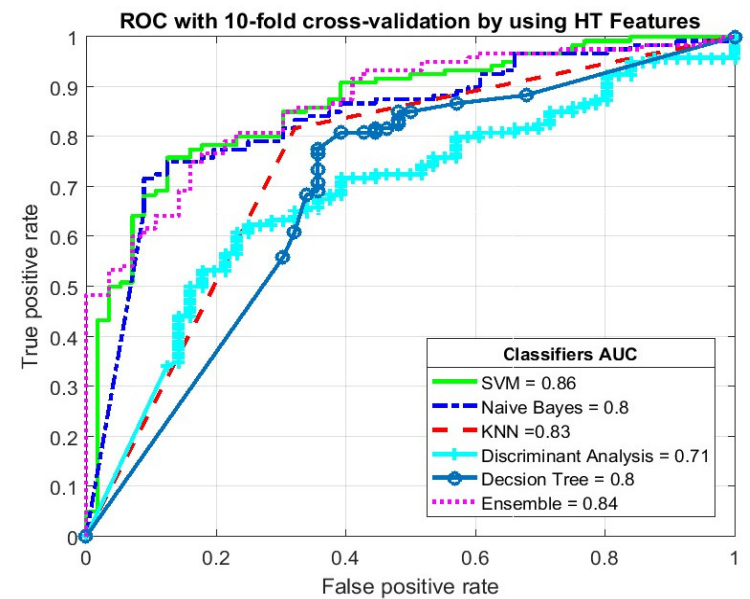


Method 1 Results

Homogeneous Texture Results

Table 4.1 Classification results by using homogeneous texture descriptors computed using the mean and standard deviation of filter responses

Classifiers	TN	FN	FP	TP	Sen	Spec	ACC	AUC
SVM	32	24	11	109	82.0%	74.4%	80.1%	0.86
NB	51	5	36	84	94.4%	58.6%	76.7%	0.80
KNN	38	18	22	98	84.5%	63.3%	77.3%	0.83
LDA	38	18	44	76	80.9%	46.3%	64.8%	0.71
DT	31	25	23	97	79.5%	57.4%	72.7%	0.80
Ensemble	39	17	21	99	85.3%	65.0%	78.4%	0.84

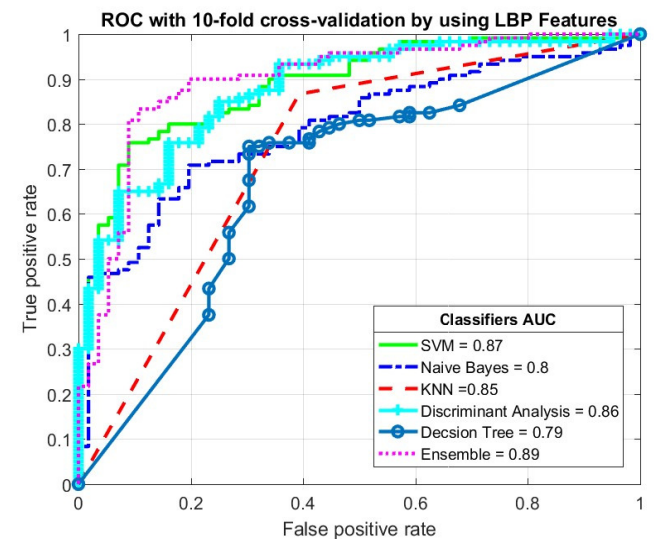


Method 1 Results

LBP Texture Results

Table 4.2: Classification results of multiple classifiers by using the LBP texture descriptors

Classifiers	TN	FN	FP	TP	Sen	Spec	ACC	AUC
SVM	29	27	7	113	80.7%	80.6%	80.7%	0.87
NB	34	22	25	95	81.2%	57.6%	73.3%	0.80
KNN	34	22	16	104	82.5%	68.0%	78.4%	0.85
LDA	42	14	18	102	87.9%	70.0%	81.8%	0.86
DT	32	24	26	94	79.7%	55.2%	71.6%	0.79
Ensemble	40	16	12	108	87.1%	76.9%	84.1%	0.89

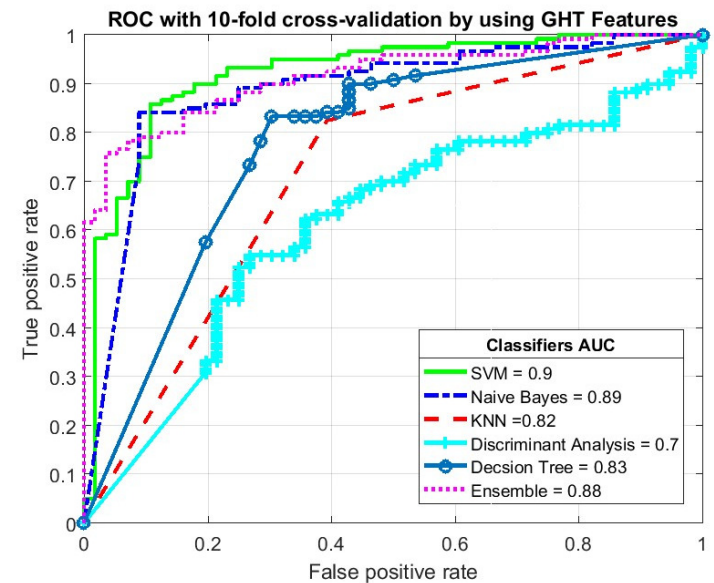


Method 1 Results

Geometric Homogenous Texture Results

Table 4.3: Classification results by using homogeneous textures descriptors computed by the geometric mean and geometric standard deviation of the filter responses

Classifiers	TN	FN	FP	TP	Sen	Spec	ACC	AUC
SVM	47	9	15	105	92.1%	75.8%	86.4%	0.90
NB	51	5	19	101	95.3%	72.9%	86.4%	0.89
KNN	34	22	21	99	81.8%	61.8%	75.6%	0.82
LDA	33	23	43	77	77.0%	43.4%	62.5%	0.70
DT	33	23	19	101	81.5%	63.5%	76.1%	0.83
Ensemble	42	14	14	106	88.3%	75.0%	84.1%	0.88

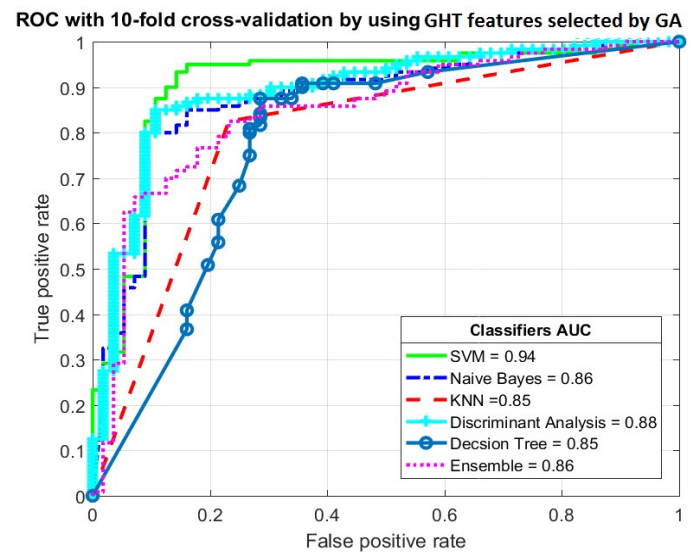


Method 1 Results

Geometric Homogenous Texture with GA Results

Table 4.4: Classification results of all the classifiers with an optimized feature selection using a genetic algorithm

Classifiers	TN	FN	FP	TP	Sen	Spec	ACC	AUC
SVM	47	9	6	114	92.7%	88.7%	91.5%	0.94
NB	50	6	24	96	94.1%	67.6%	83.0%	0.86
KNN	43	13	21	99	88.4%	67.2%	80.7%	0.85
LDA	41	15	14	106	87.6%	74.5%	83.5%	0.88
DT	44	12	19	101	89.4%	69.8%	82.4%	0.87
Ensemble	39	17	16	104	86.0%	70.9%	81.3%	0.86



Method 1 Results

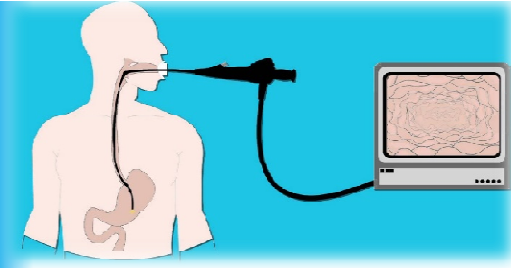
Average Accuracies Comparison



Table 4.5: Comparison of the average ACCs and AUCs with existing feature extraction methods

Classifier	Descriptors	ACC	AUC
SVM	HT [79]	81.0%	0.86
Ensemble	LBP	82.7%	0.88
SVM	GHT	86.1%	0.91
SVM	GHT with GA	90.0%	0.93





Method 2

Gastric abnormalities detection using hybrid texture descriptors for chromoendoscopy images (G2LCM)

Method 2 Results



Experimental Setup	
Parameters	Values
Features	G2LCM
Classifiers	SVM, NB, DT, LDA, Ensemble
Images	Chromoendoscopy
Validation Method	Crossover 10
Average Over	100 iterations

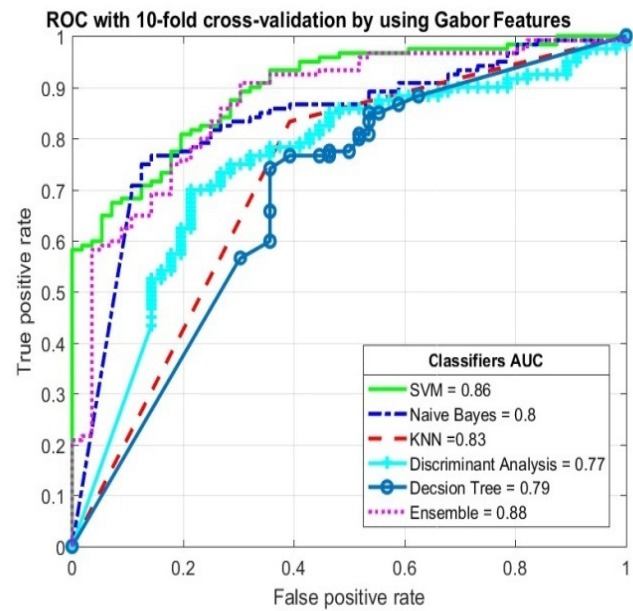


Method 2 Results

Results Homogeneous Texture

Table 4.7 Classification Performance of Multiple Classifiers by Using Homogeneous Texture Descriptors

Classifiers	TN	FN	FP	TP	Sen	Spec	ACC	AUC
SVM	40	16	17	103	87%	70%	81%	0.86
NB	49	7	35	85	92%	58%	76%	0.80
KNN	34	22	20	100	82%	63%	76%	0.83
LDA	43	13	36	84	87%	54%	72%	0.77
DT	27	29	23	97	77%	54%	70%	0.79
Ensemmble	37	19	11	109	85%	77%	83%	0.88

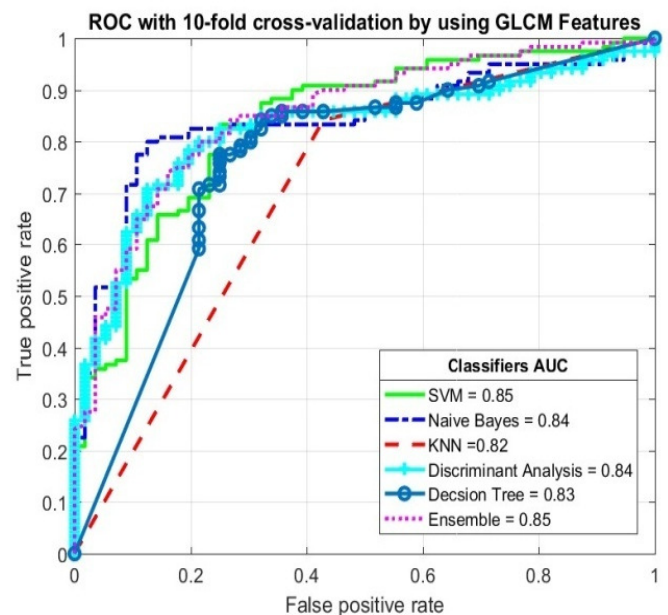


Method 2 Results

GLCM Results

Table 4.8: Classification Performance of Multiple Classifiers by Using GLCM Texture Descriptors

Classifiers	TN	FN	FP	TP	Sen	Spec	ACC	AUC
SVM	38	18	17	103	85%	69%	80%	0.85
NB	50	6	29	91	94%	63%	80%	0.84
KNN	32	24	19	101	81%	63%	76%	0.82
LDA	40	16	21	99	86%	66%	79%	0.84
DT	39	17	23	97	85%	63%	77%	0.83
Ensemble	37	19	18	102	84%	67%	79%	0.85

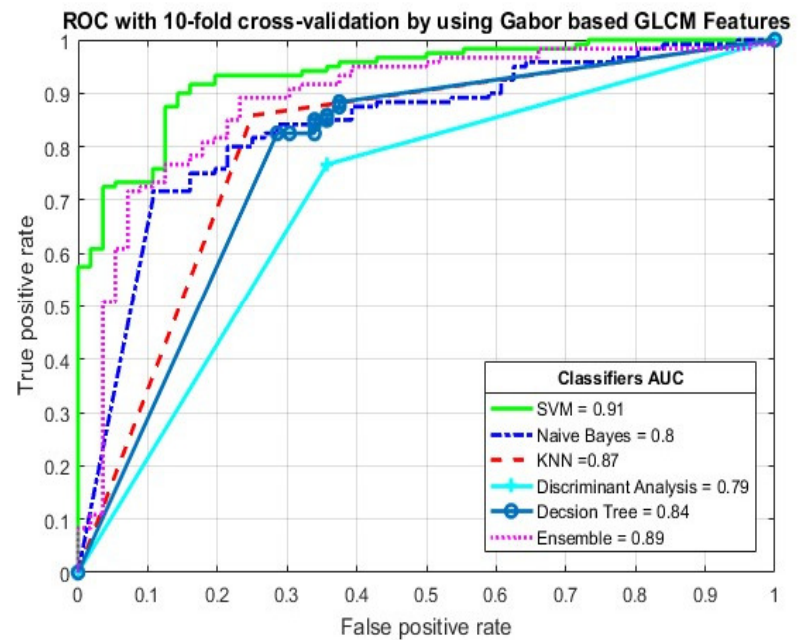


Method 2 Results

G2LCM Results

Table 4.9: Classification Performance of multiple classifiers on G2LCM descriptors

Classifiers	TN	FN	FP	TP	Sen	Spec	ACC	AUC
SVM	45	11	10	110	91%	82%	88%	0.91
NB	47	9	34	86	91%	58%	76%	0.80
KNN	42	14	17	103	88%	71%	82%	0.87
LDA	36	20	28	92	82%	56%	73%	0.79
DT	37	19	19	101	84%	66%	78%	0.84
Ensemble	43	13	14	106	89%	75%	85%	0.89

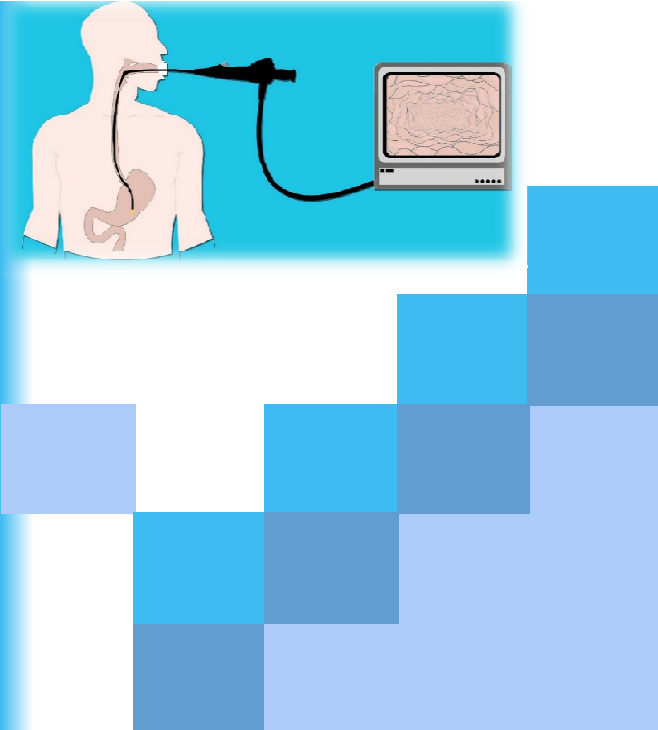


Method 2 Results

G2LCM Results

Table 4.10: Classifiers and Features Extraction Methods with highest average ACCs and AUCs

Ref.	Classifier	Descriptors	ACC	AUC
[79]	SVM	AHT	83.1%	0.85
[80]	SVM	GHT	86.1%	0.91
-	SVM	HT	81.0%	0.86
-	NB	GLCM	80.8%	0.85
Proposed	SVM	G2LCM	87.2%	0.91



Method 3

DeepGLCM and LGLCM Texture Features for Classification of Gastric Abnormalities

Method 3 Results

Experimental Setup



Experimental Setup	
Parameters	Values
Features	L-LGLCM, DeepGLCM
Classifiers	Deep Learning, Multiclass SVM
Validation Method	Crossover 10, Holdout 50%
Average Over	100 iterations
Dataset	Chromoendoscopy, Video endoscopy.
Model	AlexNet



Method 3 Results

L-GLCM Texture Features



Features	Classifiers	SVM	NB	KNN	LDA	DT	Ensemble
GLCM	ACC	$79.8\% \pm 0.2$	$80.7\% \pm 0.1$	$74.5\% \pm 0.3$	$79.6\% \pm 0.1$	$76.2\% \pm 0.4$	$77.6\% \pm 0.3$
	AUC	0.854 ± 0.002	0.844 ± 0.001	0.815 ± 0.002	0.847 ± 0.001	0.824 ± 0.003	0.838 ± 0.002
L-GLCM 2×2	ACC	$86.7\% \pm 0.2$	$83.3\% \pm 0.1$	$77.2\% \pm 0.3$	$81.5\% \pm 0.2$	$79.5\% \pm 0.4$	$84\% \pm 0.3$
	AUC	0.902 ± 0.002	0.867 ± 0.001	0.825 ± 0.002	0.864 ± 0.002	0.848 ± 0.003	0.882 ± 0.002
L-GLCM 4×4	ACC	$82.8\% \pm 0.2$	$80.6\% \pm 0.1$	$82.2\% \pm 0.2$	$77.4\% \pm 0.4$	$81\% \pm 0.4$	$83.5\% \pm 0.3$
	AUC	0.873 ± 0.002	0.847 ± 0.001	0.869 ± 0.002	0.824 ± 0.003	0.861 ± 0.003	0.88 ± 0.002
L-GLCM 8×8	ACC	$88.7\% \pm 0.2$	$81.3\% \pm 0.1$	$74.3\% \pm 0.1$	$80.5\% \pm 0.4$	$74.7\% \pm 0.6$	$83.9\% \pm 0.4$
	AUC	0.927 ± 0.001	0.852 ± 0.001	0.836 ± 0.001	0.867 ± 0.003	0.815 ± 0.005	0.883 ± 0.003



Method 3 Results

Combined LGLCM Features

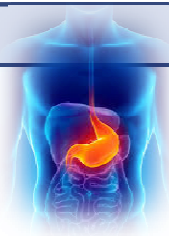


Table 4.16: A Comparison of Classification Performance of SVM Classifiers by Using L-GLCM Texture Descriptors with combination of blocks sizes

Features	TN	FN	FP	TP	Sen	Spec	ACC	AUC
GLCM	38	18	16	104	85.25%	70.37%	80.68%	0.86
LGLCM 2X2	48	8	10	110	93.22%	82.76%	89.77%	0.92
LGLCM 4X4	39	17	12	95	84.82%	76.47%	82.21%	0.87
LGLCM 8X8	15	6	3	61	91.04%	83.33%	89.41%	0.93
LGLCM (2x2 + 4x4 + 8x8)	15	12	2	76	86.36%	88.24%	86.67%	0.92
LGLCM (4X4 + 8x8)	15	12	5	73	85.88%	75.00%	83.81%	0.90
LGLCM (2x2 + 4x4)	15	12	4	74	86.05%	78.95%	84.76%	0.90
LGLCM (2x2 8x8)	15	12	3	75	86.21%	83.33%	85.71%	0.91



Method 3 Results

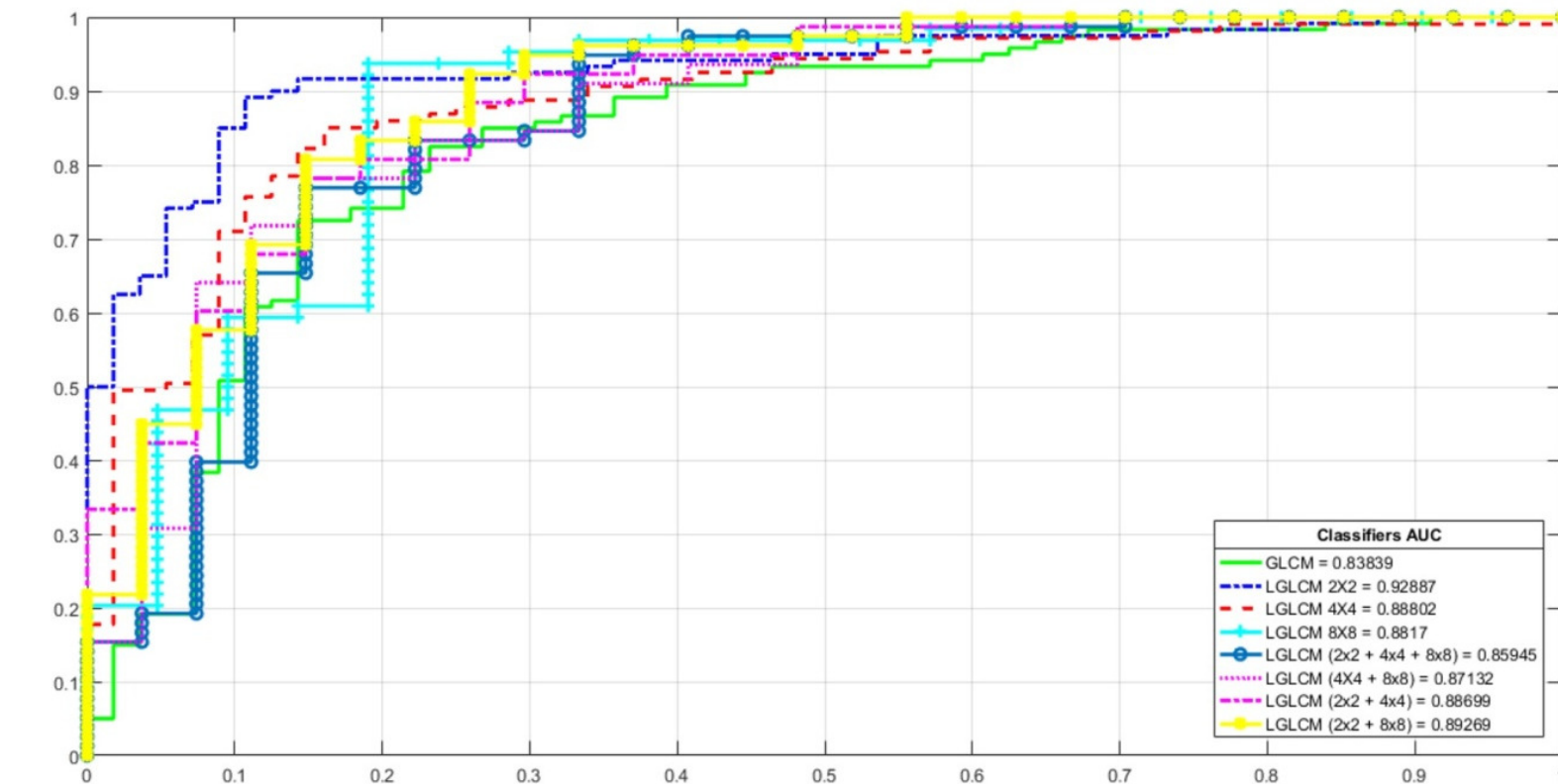


Figure 4.14: ROC and AUC of SVM Classifier using L-GLCM texture features with combination of blocks and using 10 cross validation

Method 3 Results

Different Histogram bins

Table 4.17: Classification Performance of SVM Classifier using histogram of combined locally computed GLCM (CGLCM) features by using multiple bin sizes

Features	TN	FN	FP	TP	Sen	Spec	ACC	AUC
GLCM	36	20	15	105	84.00%	70.59%	80.11%	0.86
CGLCM 10	39	17	13	107	86.29%	75.00%	82.95%	0.88
CGLCM 20	43	13	12	108	89.26%	78.18%	85.80%	0.90
CGLCM 30	45	11	13	107	90.68%	77.59%	86.36%	0.90
CGLCM 40	43	13	12	108	89.26%	78.18%	85.80%	0.90
CGLCM 50	41	15	11	109	87.90%	78.85%	85.23%	0.89
CGLCM 60	44	12	10	110	90.16%	81.48%	87.50%	0.91
CGLCM 70	42	14	17	103	88.03%	71.19%	82.39%	0.87
CGLCM 80	44	12	13	107	89.92%	77.19%	85.80%	0.90
CGLCM 90	44	12	15	105	89.74%	74.58%	84.66%	0.89

Method 3 Results

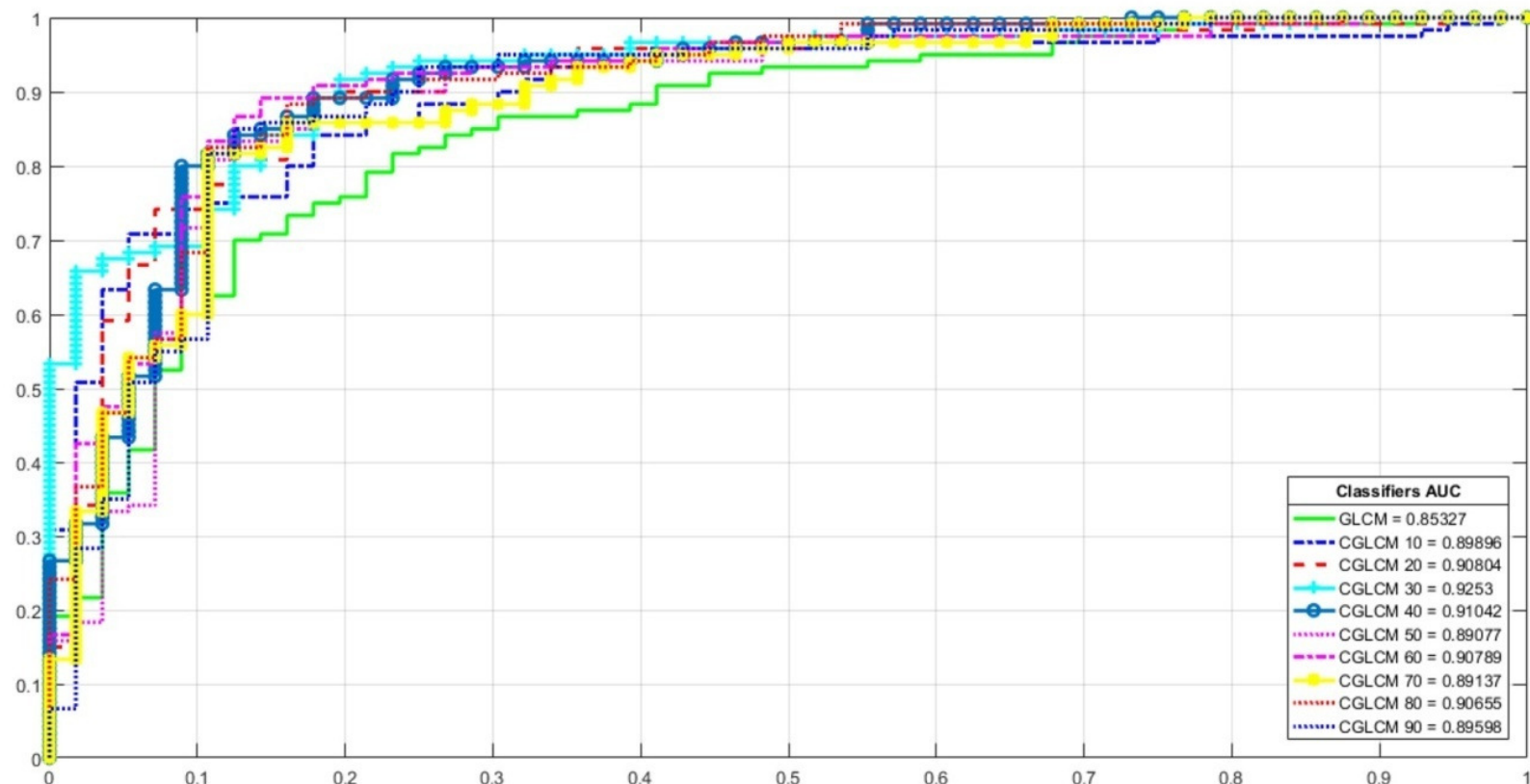


Figure 4.15: ROC and AUC of SVM Classifier using CGLCM histogram texture features with different bin sizes and using 10 cross validation

Method 3 Results

DeepGLCM Texture descriptors



Layer	Classifier	SVM	NB	KNN	LDA	DT	Ensemble
Conv1	ACC	$87.3\% \pm 0.2$	$81.8\% \pm 0.1$	$89.4\% \pm 0.2$	$86.8\% \pm 0.3$	$80.6\% \pm 0.5$	$90.4\% \pm 0.2$
	AUC	0.784 ± 0.003	0.74 ± 0.001	0.822 ± 0.004	0.789 ± 0.006	$2.5\% \pm 196$	0.845 ± 0.004
Conv2	ACC	$89.8\% \pm 0.2$	$81.5\% \pm 0.1$	$89.4\% \pm 0.2$	$94.3\% \pm 0.2$	$78.9\% \pm 0.5$	$90.6\% \pm 0.3$
	AUC	0.829 ± 0.004	0.703 ± 0.002	0.838 ± 0.003	0.91 ± 0.003	0.664 ± 0.008	0.848 ± 0.005
Conv3	ACC	$88\% \pm 0.2$	$77.7\% \pm 0.1$	$90.9\% \pm 0.2$	$92.3\% \pm 0.2$	$76.2\% \pm 0.5$	$90.9\% \pm 0.2$
	AUC	0.788 ± 0.004	0.625 ± 0.002	0.865 ± 0.003	0.876 ± 0.004	0.627 ± 0.008	0.851 ± 0.004
Conv4	ACC	$85.9\% \pm 0.2$	$80.4\% \pm 0.2$	$87.7\% \pm 0.2$	$93.9\% \pm 0.2$	$73.8\% \pm 0.5$	$87.2\% \pm 0.3$
	AUC	0.737 ± 0.004	0.661 ± 0.004	0.828 ± 0.003	0.9 ± 0.004	0.597 ± 0.009	0.781 ± 0.005
Conv5	ACC	$84.3\% \pm 0.2$	$81.6\% \pm 0.2$	$82.8\% \pm 0.2$	$85.6\% \pm 0.3$	$74.6\% \pm 0.5$	$84.2\% \pm 0.3$
	AUC	0.698 ± 0.004	0.687 ± 0.004	0.74 ± 0.003	0.758 ± 0.005	0.605 ± 0.007	0.723 ± 0.006



Method 3 Results

DeepGLCM Texture Descriptors Comparison



Ref.	Classifier	Descriptors	ACC	AUC
[79]	SVM	AHT	83.1%	0.85
[81]	SVM	G2LCM	87.2%	0.91
[80]	SVM	GHT	86.1%	0.91
	SVM	HT	81.0%	0.86
	Ensemble	LBP	82.7%	0.88
[82]	NB	GLCM	80.7%	0.84
Proposed	SVM	L-GLCM (2×2)	86.7%	0.90
	Ensemble	L-GLCM (4×4)	83.5%	0.88
	SVM	CGLCM 30	86.2%	0.90
	SVM	CGLCM 60	87.1%	0.91
	SVM	L-GLCM (8×8)	88.7%	0.92
	LDA	DeepGLCM (Conv2)	94.3%	0.92



Method 3 Results

DeepGLCM 1st layer

Table 4.24: Results of Multiclass SVM classifier by using DeepGLCM on 1st layer of DCNN on Video Endoscopy Datasae with 8 class labels

True Class	Class	A	B	C	D	E	F	G	H	Sen
	A	308	164	0	2	0	0	21	5	62%
	B	172	306	0	2	0	0	16	4	61%
	C	1	0	378	0	10	111	0	0	76%
	D	1	1	0	421	0	0	59	18	84%
	E	0	0	10	0	464	17	4	5	93%
	F	1	0	91	0	14	393	0	1	79%
	G	2	1	3	47	17	1	346	83	69%
	H	4	1	0	23	7	1	89	375	75%
	Pre	63%	65%	78%	85%	91%	75%	65%	76%	



Method 3 Results

DeepGLCM on 2nd layer

Table 4.25: Results of Multiclass SVM classifier by using DeepGLCM on 2nd layer of DCNN on Video Endoscopy Dataset with 8 class labels

True Class	Class	A	B	C	D	E	F	G	H	Sen
	A	379	103	0	0	0	0	15	3	76%
	B	118	376	0	0	0	0	6	0	75%
	C	0	0	395	0	1	103	1	0	79%
	D	0	0	0	461	0	0	36	3	92%
	E	0	0	2	0	483	6	7	2	97%
	F	0	0	68	0	7	423	1	1	85%
	G	2	0	1	26	17	1	416	37	83%
	H	2	0	1	11	4	1	39	442	88%
	Pre	76%	78%	85%	93%	94%	79%	80%	91%	
		Predicted Class								



Method 3 Results

DeepGLCM on 3rd layer

Table 4.26: Results of Multiclass SVM classifier by using DeepGLCM on 3rd layer of DCNN on Video Endoscopy Dataset with 8 class labels

	Class	A	B	C	D	E	F	G	H	Sen
True Class	A	358	119	0	0	0	0	18	5	72%
	B	136	358	0	1	0	0	4	1	72%
	C	0	0	402	0	0	98	0	0	80%
	D	0	0	0	455	0	0	38	7	91%
	E	0	1	2	0	488	7	0	2	98%
	F	1	0	60	0	3	431	4	1	86%
	G	2	0	4	18	12	2	437	25	87%
	H	2	1	1	9	4	1	46	436	87%
	Pre	72%	75%	86%	94%	96%	80%	80%	91%	
		Predicted Class								



Method 3 Results

DeepGLCM on 4th layer

Table 4.27: Results of Multiclass SVM classifier by using DeepGLCM on 4th layer of DCNN on Video Endoscopy Dataset with 8 class labels

True Class	Class	A	B	C	D	E	F	G	H	Sen
	A	358	119	0	0	0	0	18	5	72%
	B	136	358	0	1	0	0	4	1	72%
	C	0	0	402	0	0	98	0	0	80%
	D	0	0	0	455	0	0	38	7	91%
	E	0	1	2	0	488	7	0	2	98%
	F	1	0	60	0	3	431	4	1	86%
	G	2	0	4	18	12	2	437	25	87%
	H	2	1	1	9	4	1	46	436	87%
	Pre	72%	75%	86%	94%	96%	80%	80%	91%	
		Predicted Class								

Method 3 Results

DeepGLCM on 5th layer

Table 4.28: Results of Multiclass SVM classifier by using DeepGLCM on 5th layer of DCNN on Video Endoscopy Dataset with 8 class labels

True Class	Class	A	B	C	D	E	F	G	H	Sen
	A	368	114	0	1	0	0	15	2	74%
	B	122	368	0	2	0	0	7	1	74%
	C	0	0	401	0	1	94	4	0	80%
	D	0	0	0	463	0	0	28	9	93%
	E	0	0	7	0	478	4	9	2	96%
	F	0	0	66	0	4	428	1	1	86%
	G	8	0	3	20	14	0	437	18	87%
	H	0	2	1	9	6	0	40	442	88%
	Pre	74%	76%	84%	94%	95%	81%	81%	93%	
		Predicted Class								



Method 3 Results

Deep-GLCM



Table 4.29: Average Results of Multiclass SVM classifier by using DeepGLCM on 5 layers of DCNN on Video Endoscopy Dataset with 8 class labels

Features	DeepGLCM Texture	
Layers	ACC	AUC
Conv1	75.5%±0.1	0.97±0.000
Conv2	84.0%±0.1	0.99±0.000
Conv3	84.2%±0.0	0.99±0.000
Conv4	84.1%±0.0	0.99±0.000
Conv5	84.6%±0.0	0.99±0.000



Method 3 Results

Deep-GLCM

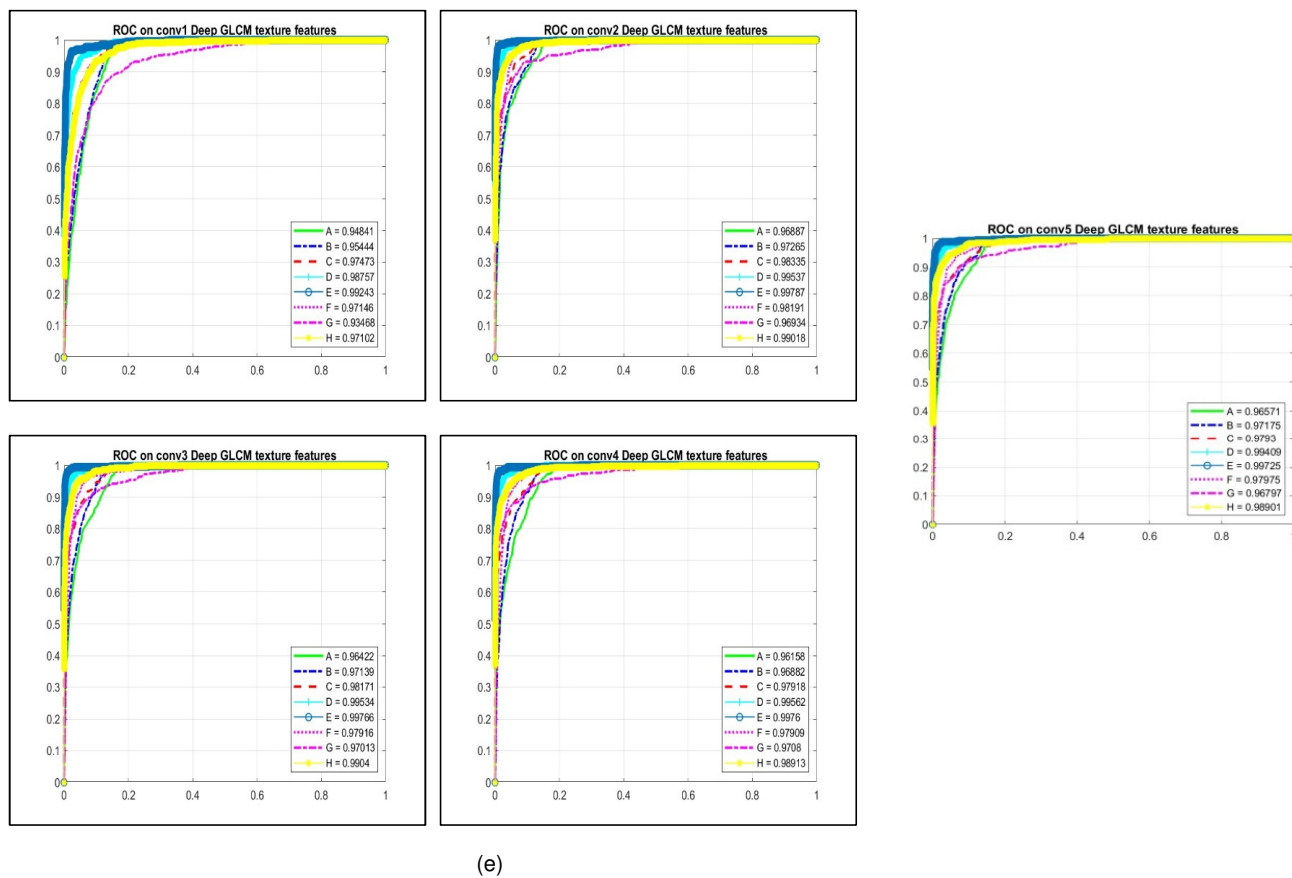
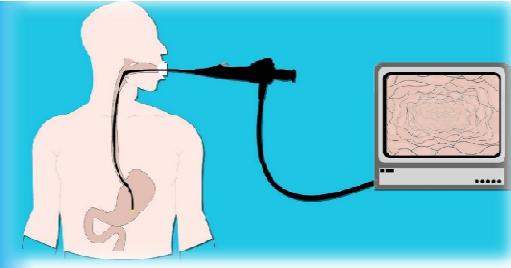


Figure 4.21: AUC and ROC of DeepGLCM on kvasir Dataset (a) 1st layer, (b) 2nd layer, (c) 3rd layer, (d) 4th layer, and (e) 5th layer training a multi class SVM



Method 4

Color-based Template Selection for Detection of Gastric Abnormalities in Video Endoscopy

Method 4 Results

Color and Color-Texture

Table 4.35: Average Accuracy and AUC of SVM classifier over multiple colors and color-texture features for classification of lesion level and image level CH images

Classification	Image Level				Lesion Level			
	Colors		Color-Texture		Colors		Color-Texture	
Features	ACC	AUC	ACC	AUC	ACC	AUC	ACC	AUC
Channels								
RGB	84.5%±0.2	0.90±0.001	82.8%±0.2	0.88±0.001	82.4%±0.2	0.88±0.001	80.4%±0.2	0.86±0.002
R	83.8%±0.2	0.89±0.001	84.1%±0.2	0.88±0.001	86.3%±0.2	0.91±0.001	78.8%±0.3	0.85±0.002
G	80.0%±0.2	0.87±0.001	79.7%±0.3	0.86±0.002	79.7%±0.2	0.86±0.001	75.9%±0.3	0.83±0.002
B	81.3%±0.1	0.88±0.001	81.6%±0.2	0.87±0.002	79.6%±0.2	0.87±0.001	77.6%±0.3	0.84±0.002
HSV	85.8%±0.2	0.90±0.001	82.5%±0.2	0.88±0.002	85.0%±0.2	0.90±0.001	82.7%±0.3	0.88±0.002
H	85.1%±0.3	0.90±0.002	77.3%±0.2	0.85±0.001	86.6%±0.2	0.91±0.002	77.6%±0.2	0.85±0.002
S	74.2%±0.2	0.83±0.002	83.6%±0.2	0.88±0.002	77.7%±0.3	0.85±0.002	81.4%±0.3	0.86±0.002
V	83.2%±0.2	0.89±0.002	81.1%±0.2	0.87±0.002	80.9%±0.3	0.87±0.002	77.6%±0.3	0.84±0.002
Lab	84.2%±0.1	0.89±0.001	81.0%±0.2	0.87±0.001	79.8%±0.1	0.86±0.001	80.3%±0.2	0.86±0.001
L	81.4%±0.1	0.88±0.001	73.6%±0.2	0.84±0.001	67.0%±0.4	0.79±0.003	68.1%±0.2	0.81±0.001
a	79.8%±0.2	0.86±0.001	78.0%±0.1	0.85±0.001	77.4%±0.2	0.84±0.001	76.5%±0.1	0.83±0.001
b	80.6%±0.1	0.87±0.001	74.4%±0.2	0.83±0.001	78.7%±0.1	0.86±0.000	78.3%±0.2	0.85±0.001
YCbCr	80.3%±0.2	0.87±0.001	85.3%±0.2	0.89±0.002	80.3%±0.2	0.87±0.002	83.4%±0.2	0.88±0.002
Y	83.3%±0.2	0.89±0.001	82.0%±0.2	0.87±0.001	81.6%±0.3	0.87±0.002	79.5%±0.3	0.85±0.002
Cb	81.2%±0.2	0.87±0.001	79.1%±0.2	0.86±0.001	81.4%±0.2	0.88±0.001	77.8%±0.3	0.84±0.002
Cr	81.0%±0.2	0.87±0.001	78.4%±0.2	0.85±0.002	81.1%±0.2	0.87±0.002	77.0%±0.3	0.84±0.002
XYZ	82.8%±0.2	0.88±0.001	82.9%±0.1	0.88±0.001	83.3%±0.2	0.89±0.001	82.8%±0.2	0.88±0.001
X	82.6%±0.2	0.88±0.001	84.7%±0.2	0.89±0.001	82.9%±0.2	0.88±0.001	84.3%±0.2	0.89±0.001
Y	82.1%±0.2	0.88±0.001	85.9%±0.2	0.90±0.001	80.2%±0.2	0.87±0.001	84.5%±0.2	0.89±0.001
Z	79.7%±0.1	0.87±0.001	78.5%±0.2	0.85±0.002	79.9%±0.1	0.87±0.001	75.5%±0.3	0.84±0.002

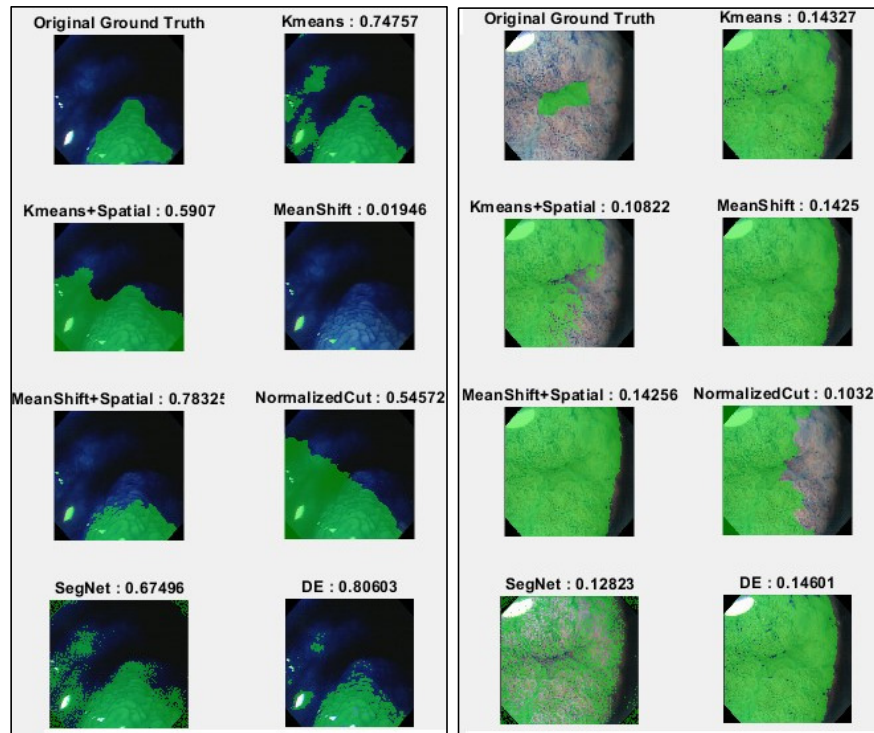




Table 4.36: Average segmentation results comparison with existing segmentation methods

Methods	Average DSC	Average ACC
Kmean (Color) [85]	0.4739	56.24%
Kmean (Color + Spatial) [86]	0.4798	54.56%
Mean-shift (Color) [88]	0.3770	53.67%
Mean-shift (Color + Spatial) [89]	0.4073	54.80%
Normalized Cut (Color) [87]	0.5200	55.73%
SegNet [90]	0.2905	29.45%
ΔE Manual	0.5187	57.44%
ΔE Automatic	0.5063	56.88%





Computer-aided Analysis of Endoscopic-frames for the
Detection of Abnormalities in Gastrointestinal Tract

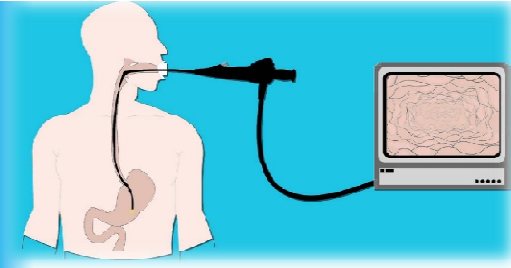




- Table 4.37: Features Extraction Methods with Highest Average ACCs and AUCs

Ref.	Descriptors	ACC	AUC
[79]	AHT	83.1%	0.85
[90]	GHT	86.1%	0.91
Image-Level	XYZ Color-Texture	86.1%	0.90
Lesion- Level	HSV Color	86.6%	0.91





Method 5

Computer-aided Analysis of Endoscopic-frames for the Detection of Abnormalities in
Gastrointestinal Tract



Table 4.39: Average classification performance of CNN on VE and CH data sets

Data sets	Classification Level	Training Options		Sensitivity	Classification Performance		AUC
		Ephocs	Batch-size		Specificity	Accuracy	
CH	Lesion	10	10	87.2% \pm 1.1	96.7% \pm 0.6	93.3% \pm 0.6	0.898 \pm 0.009
	Image	20	20	91.6% \pm 1	86.3% \pm 0.8	87.3% \pm 0.8	0.762 \pm 0.019
VE	Lesion	20	20	80.9% \pm 0.8	76.7% \pm 0.4	78.5% \pm 0.4	0.778 \pm 0.004
	Image	10	10	55.2% \pm 0.9	50.6% \pm 0.4	52.2% \pm 0.5	0.445 \pm 0.005
CH & VE	Lesion	5	10	52.5% \pm 0.4	97.8% \pm 0.5	63.2% \pm 0.5	0.685 \pm 0.003
	Whole	30	20	46.7% \pm 0.1	100% \pm 0	53.2% \pm 0.1	0.637 \pm 0.001





Ref.	Classifier	Descriptors	ACC
[79]	SVM	AHT	83.1%
[81]	SVM	G2LCM	87.2%
	SVM	GHT	86.1%
[80]	SVM	HT	81.0%
	Ensemble	LBP	82.7%
CNN- Image Level			87.3%
CNN- Lesion Level			93.3%



Outline



1. Introduction
2. Literature Review
3. Challenges
4. Problem Statement
5. Proposed Methods
6. Results and Discussions
7. Conclusion and Future Work
8. Contributions
9. References
10. Questions Answers



Conclusion



- **Texture features** exhibited a good performance in terms of discrimination on the CH images. The experimental results showed the significance of GHT features with and without feature selection.
- **SVM classifier** with best performance among other state-of-the-art classifiers.
- **Hybrid Texture features** such as DeepGLCM and G2LCM have greater performance.
- Also, locally computed textures **LGLCM** have better performance than globally computed features .



Conclusion

- In endoscopy frames RGB color space is not well-utilized.
- HSV and Lab color spaces are helpful in both classification and segmentation of gastric images.
- Deep learning achieved best classification accuracy in both ways using transfer leaning and feature learning using layer activation.



Future Directions



- These features can also be used for the classification of images of other endoscopy modalities.
- In future, it would be interesting to use color features with other texture extraction method to achieve an optimum accuracy for classification.
- Nano wire based endoscopes and optical fiber photonic crystal based endoscope. These devices can perform the intra-cellular sensing of enzymes, gastric pH level, calcium ions, carcinogens, biomarkers, and quantum dots using fluorescence in early detection of gastric cancer



Outline

1. Introduction
2. Literature Review
3. Challenges
4. Problem Statement
5. Proposed Methods
6. Results and Discussions
7. Conclusion and Future Work
8. Contributions
9. References
10. Questions Answers



Contributions

Hussam Ali, Muhammad Sharif, Mussarat Yasmin, and Mubashir Husain Rehmani.
"Computer-based classification of chromoendoscopy images using homogeneous texture descriptors."
Computers in biology and medicine 88 (2017): 84-92. [Impact Factor 2.11].



Computer-based classification of chromoendoscopy images using homogeneous texture descriptors

Hussam Ali ^{a,*}, Muhammad Sharif^a, Mussarat Yasmin^a, Mubashir Husain Rehmani^b

^aDepartment of Computer Science, COMSATS Institute of Information Technology, Wah Cantt, Pakistan

^bDepartment of Electrical Engineering, COMSATS Institute of Information Technology, Wah Cantt, Pakistan

ARTICLE INFO

Keywords:
Classification
Endoscopy
Feature extraction
Gastrointestinal
Gastric cancer
Local binary patterns
Homogeneous texture
Chromoendoscopy
Genetic algorithm

ABSTRACT

Computer-aided analysis of clinical pathologies is a challenging task in the field of medical imaging. Specifically, the detection of abnormal regions in the frames collected during an endoscopic session is difficult. The variations in the conditions of image acquisition, such as field of view or illumination modification, make it more demanding. Therefore, the design of a computer-assisted diagnostic system for the recognition of gastric abnormalities requires features that are robust to scale, rotation, and illumination variations of the images. Therefore, this study focuses on designing a set of texture descriptors based on the Gabor wavelets that will cope with certain image dynamics. The proposed features are extracted from the images and utilized for the classification of the chromoendoscopy (CH) frames into normal and abnormal categories. Moreover, to attain a higher accuracy, an optimized subset of descriptors is selected through the genetic algorithm. The results obtained using the proposed features are compared with other existing texture descriptors (e.g., local binary pattern and homogeneous texture descriptors). In addition, the selected features are used to train the support vector machine (SVM), naive Bayes (NB) algorithm, k-nearest neighbor algorithm, linear discriminant analysis, and ensemble tree classifier. The performance of these state-of-the-art classifiers for different texture descriptors is compared based on the accuracy, sensitivity, specificity, and area under the curve (AUC) derived by using the CH images. The classification results reveal that the SVM classifier achieves 90.0% average accuracy and 0.93 AUC when it is employed with an optimized set of features obtained by using a genetic algorithm.

1. Introduction

In recent years, there has been an increase in the concern for gastric cancer globally [1]. An inappropriate diet is one of the main causes of complications (e.g., ulcer and inflammation) in the gastrointestinal (GI) tract [2]. In addition, these abnormalities may contribute to the development of gastric cancer [3].

An early diagnosis of tumors is useful for decreasing the mortality rate [4]. For the well-timed detection of tumors, a normal clinical practice is intestinal biopsy (in which tissue samples of the mucosa are collected and analyzed) conducted by an expert to identify if there are any cancerous or abnormal cells present in the tissue samples [5]. In contrast, endoscopy is a less invasive method for screening the GI tract. An endoscope is composed of a flexible tube with a mounted camera, light source, and surgical apparatus [6]. Therefore, an endoscope is also sometimes used for performing GI biopsies [7]. Inspection of the GI tract via an endoscope

is an indispensable task for the timely identification of irregularities (e.g., cancer, ulcer, and polyps) in gastric patients. Various improvements have been made in the video endoscopy technology [8]. Chromoendoscopy (CH) is an advancement of video endoscopy [9]. CH facilitates the investigation of mucosal vascular structures by spraying dyes over the mucosal surface. The dyes make the cancerous regions more prominent visually, and several clinical studies have also utilized their benefits. Digital (virtual) CH employs image processing algorithms and uses band-pass filters to render the effect of dye-based (traditional) CH. The advantage of virtual CH over traditional CH is that there is no requirement of spraying colorants. Therefore, there is no necessity for extra cleansing that is otherwise essential before performing further endoscopic procedures [10]. An endoscopic procedure performed for a single patient can consume 45 min to 8 h of time, producing more than 80,000 frames. However, majority of the frames are discarded because of degradation or high-similarity between them. Thus, for a physician it is a

* Corresponding author.
E-mail addresses: hussamalics@gmail.com (H. Ali), mohammadsharifmalik@yahoo.com (M. Sharif), mussaratabdullah@gmail.com (M. Yasmin), mshrehmani@gmail.com (M.H. Rehmani).

<https://doi.org/10.1016/j.combiomed.2017.07.002>

Received 17 February 2017; Received in revised form 29 June 2017; Accepted 2 July 2017

0010-4825/© 2017 Elsevier Ltd. All rights reserved.

Computer-aided Analysis of Endoscopic-frames for the
Detection of Abnormalities in Gastrointestinal Tract



Contributions

Hussam Ali, Mussarat Yasmin, Muhammad Sharif, and Mubashir Husain Rehmani.
"Computer Assisted Gastric Abnormalities Detection Using Hybrid Texture Descriptors for Chromoendoscopy Images." Computer Methods and Programs in Biomedicine (2018). [Impact Factor 3.4].

Computer Methods and Programs in Biomedicine 157 (2018) 39–47



Contents lists available at ScienceDirect

Computer Methods and Programs in Biomedicine

journal homepage: www.elsevier.com/locate/cmpb



Computer assisted gastric abnormalities detection using hybrid texture descriptors for chromoendoscopy images



Hussam Ali^{a,*}, Mussarat Yasmin^a, Muhammad Sharif^a, Mubashir Husain Rehmani^b

^a COMSATS Institute of Information Technology Wah, Pakistan

^b Telecommunications Software and Systems Group (TSSG) Waterford Institute of Technology (WIT), Ireland

ARTICLE INFO

Article history:

Received 17 June 2017

Revised 25 November 2017

Accepted 10 January 2018

Keywords:

Chromoendoscopy
Co-occurrence matrix
Filter bank
Texture analysis
Gabor filter
Stomach cancer

ABSTRACT

Background and Objective: The early diagnosis of stomach cancer can be performed by using a proper screening procedure. Chromoendoscopy (CH) is an image-enhanced video endoscopy technique, which is used for inspection of the gastrointestinal-tract by spraying dyes to highlight the gastric mucosal structures. An endoscopy session can end up with generating a large number of video frames. Therefore, inspection of every individual endoscopic-frame is an exhaustive task for the medical experts. In contrast with manual inspection, the automated analysis of gastroenterology images using computer vision based techniques can provide assistance to endoscopist, by finding out abnormal frames from the whole endoscopic sequence.

Methods: In this paper, we have presented a new feature extraction method named as Gabor-based gray-level co-occurrence matrix (G2LCM) for computer-aided detection of CH abnormal frames. It is a hybrid texture extraction approach which extracts a combination both local and global texture descriptors. Moreover, texture information of a CH image is represented by computing the gray level co-occurrence matrix of Gabor filters responses. Furthermore, the second-order statistics of these co-occurrence matrices are computed to represent images' texture.

Results: The obtained results show the possibility to correctly classifying abnormal from normal frames, with sensitivity, specificity, accuracy, and area under the curve as 91%, 82%, 87% and 0.91 respectively, by using a support vector machine classifier and G2LCM texture features.

Conclusion: It is apparent from results that the proposed system can be used for providing aid to the gastroenterologist in the screening of the gastric tract. Ultimately, the time taken by an endoscopic procedure will be sufficiently reduced.

© 2018 Elsevier B.V. All rights reserved.

Computer-aided Analysis of Endoscopic-frames for the
Detection of Abnormalities in Gastrointestinal Tract



Contributions

Hussam Ali, Mussarat Yasmin, Muhammad Sharif, Mubashir Husain Rehmani, and Farhan Riaz, A Survey of Feature Extraction and Fusion of Deep Learning for Detection of Abnormalities in Video Endoscopy of Gastrointestinal-tract, has been accepted for publication in Artificial Intelligence Review , 2019 . [ISI Indexed, Impact Factor: 5.095]

A survey of feature extraction and fusion of deep learning for detection of abnormalities in video endoscopy of gastrointestinal-tract

**Hussam Ali, Muhammad Sharif,
Mussarat Yasmin, Mubashir Husain
Rehmani & Farhan Riaz**

Artificial Intelligence Review
An International Science and
Engineering Journal
ISSN 0269-2821
Artif Intell Rev
DOI 10.1007/s10462-019-09743-2



Springer

Computer-aided Analysis of Endoscopic-frames for the
Detection of Abnormalities in Gastrointestinal Tract

113



Contributions

- Hussam Ali, Mussarat Yasmin, Muhammad Sharif, and Mubashir Husain Rehmani, Color-based Template Selection for Detection of Gastric Abnormalities in Video Endoscopy, has been accepted for publication in Biomedical Signal Processing and Control , 2020 . [ISI Indexed, Impact Factor: 2.9]

Biomedical Signal Processing and Control 56 (2020) 101668

Contents lists available at ScienceDirect

Biomedical Signal Processing and Control

journal homepage: www.elsevier.com/locate/bspc



Color-based template selection for detection of gastric abnormalities in video endoscopy

Hussam Ali^a, Muhammad Sharif^a, Mussarat Yasmin^a, Mubashir Husain Rehmani^b

^aDepartment of Computer Science, COMSATS University Islamabad, Wah Campus, Pakistan

^bDepartment of Computer Science, Cork Institute of Technology (CIT), Ireland

ARTICLE INFO

Article history:
Received 8 July 2018
Received in revised form 16 July 2019
Accepted 17 August 2019
Available online 9 November 2019

Keywords:
Abnormality detection
Computer aided diagnosis (CAD)
Color histogram
Segmentation
Endoscopy
Support vector machine (SVM)

ABSTRACT

Computer-aided diagnosis of gastric diseases from endoscopy frames is an important task. It facilitates both the patient and gastroenterologist in terms of time, money and most important health. Colors are the basic visual features of endoscopic images and also provide clues about abnormal regions in endoscopy frames. A variety of color spaces are available for representation of color frames. However, we are not certain about which color space is more suitable for representing color features of gastric images. This paper presents a comparison of color features in different color spaces for detection of abnormal areas in chroendoendoscopy (CH) frames. In addition, the CH images are segmented by using an existing color difference based segmentation method Delta E (ΔE). A framework for automatic segmentation is presented for endoscopy images by combining a color difference based ΔE by using SVM model. For classification colors features are used with texture descriptors. The using vector in the SVM model is trained on color features and also the hybrid color combined texture characteristics. Then the trained classifier is used to group CH frames into abnormal and normal classes. With manual template selection has achieved 57.44% accuracy and 56.88% accuracy with the automated process. Moreover, the suggested method achieves 86.6% accuracy and 0.91 area under the curve for the classification of gastric lesions.

© 2019 Elsevier Ltd. All rights reserved.

1. Introduction

Video endoscopy is a normal procedure for screening the gastrointestinal (GI) tract of a patient for potential abnormalities e.g., cancer, ulcer, and bleeding. An endoscope is not more than a wire with a light source and camera mounted on its distal tip [1]. However, the interpretation of the gastrointestinal (GI) tract (or endoscopy) is a time spending and tedious task for the medical experts. In fact, video endoscopy generates a large number of frames which are then carefully examined by a gastroenterologist [2]. An automated vision-based system can play an important role by searching out malignant frames from all video frames which saves time for the medical experts, especially when medical experts have to screen too many patients [3].

Numerous improvements have been made in the simple white light endoscopy to provide easiness to the gastroenterologist. These advancements highlight the abnormal regions on the mucosal surface and to make them more prominent to the medical experts [4].

The extraction of important characteristics from medical images is an important step for detection of abnormalities in a computer-aided diagnosis system. Colors are one of the vital and basic visual descriptors for the detection of gastric abnormalities [7]. Many studies confirm their role in the detection of abnormal frames in an endoscopic sequence [8–10]. The visual description of abnormalities (e.g., bleeding and ulcer) can be efficiently manifested by color features. Color images are represented in a combination of color channels in specific color spaces and CH frames also consist of three color channels: red, green and blue (RGB). Some well-known color spaces are hue, saturation, & value (HSV), cyan, magenta, yellow, & black (CMYK), XYZ and Lab defined by which is the International Commission on Illumination (CIE). There are many more color spaces and every color space has its own application-specific advantages.

E-mail addresses: hussamali@gsu.edu.sa (H. Ali), muhammadsharifmail@yahoo.com (M. Sharif), mmscarababullah@gmail.com (M. Yasmin), mshrehmani@gmail.com (M.H. Rehmani).

<https://doi.org/10.1016/j.bspc.2019.101668>
1746-8094/© 2019 Elsevier Ltd. All rights reserved.

Outline

1. Introduction
2. Literature Review
3. Challenges
4. Problem Statement
5. Proposed Methods
6. Results and Discussions
7. Conclusion and Future Work
8. Contributions
9. References
10. Questions Answers



References

1. P. Shanmuga Sundaram and N. Santhiyakumari. An Enhancement of Computer Aided Approach for Colon Cancer Detection in WCE Images Using ROI Based Color Histogram and SVM2. *Journal of Medical Systems*, 43(2), 2019.
2. Ouiem Bchir, Mohamed Maher Ben Ismail, and Nada AlZahrani. Multiple bleeding detection in wireless capsule endoscopy. *Signal, Image and Video Processing*, 13(1):121–126, 2019.
3. Konstantin Pogorelov, Shipra Suman, Fawnizu Azmadi Hussin, Aamir Saeed Malik, Olga Ostroukhova, Michael Riegler, Pal Halvorsen, Shiaw Hooi Ho, and Khean-Lee Goh. Bleeding detection in wireless capsule endoscopy videoscolor versus texture features. *Journal of applied clinical medical physics*, 2019.
4. Farah Deeba, Monzurul Islam, Francis M. Bui, and Khan A. Wahid. Performance assessment of a bleeding detection algorithm for endoscopic video based on classifier fusion method and exhaustive feature selection. *Biomedical Signal Processing and Control*, 40:415–424, 2018.
5. Tonmoy Ghosh, Shaikh Anowarul Fattah, and Khan A. Wahid. CHOBS: Color Histogram of Block Statistics for Automatic Bleeding Detection in Wireless Capsule Endoscopy Video. *IEEE Journal of Translational Engineering in Health and Medicine*, 6(May 2017), 2018.
6. Sergio E. Martinez-Herrera, Yannick Benezeth, Matthieu Boffety, Jean François Emile, Franck Marzani, Dominique Lamarque, and François Goudail. Identification of precancerous lesions by multispectral gastroendoscopy. *Signal, Image and Video Processing*, 10(3):455–462, 2016.
7. Pedro M Vieira, Jaime Ramos, and Carlos S Lima. Automatic detection of small bowel tumors in endoscopic capsule images by roi selection based on discarded lightness information. In *37th Annual International Conference of the IEEE on Engineering in Medicine and Biology Society (EMBC)*, pages 3025–3028, 2015.
8. Yixuan Yuan and M.Q.-H. Meng. Automatic bleeding frame detection in the wireless capsule endoscopy images. In *IEEE International Conference on Robotics and Automation, ICRA*, pages 1310–1315, 2015.
9. Dimitris K Iakovidis, Dimitris Chatzis, Panos Chrysanthopoulos, and Anastasios Koulaouzidis. Blood detection in wireless capsule endoscope images based on salient superpixels. In *Annual International Conference of the IEEE Engineering in Medicine and Biology Society (EMBS)*, pages 731–734, 2015.
10. SOUAIDI Meryem and Mohamed El Ansari. Multi-scale analysis of ulcer disease detection from wireless capsule endoscopy images. *IET Image Processing*, 2019.

References



11. Said Charfi and Mohamed El Ansari. A locally based feature descriptor for abnormalities detection. *Soft Computing*, 2019.
12. Yongsheng Dong, Jinwang Feng, Chunlei Yang, Xiaohong Wang, Lintao Zheng, and Jiexin Pu. Multi-scale counting and difference representation for texture classification. *The Visual Computer*, 34(10):1315–1324, 2018.
13. Ashok Dahal, Junghwan Oh, Wallapak Tavanapong, Johnny Wong, and Piet C. De Groen. Detection of ulcerative colitis severity in colonoscopy video frames. *International Workshop on Content-Based Multimedia Indexing*, 2015.
14. Adriana Florentina Constantinescu, Mihaela Ionescu, Ion Rogoveanu, Marius Eugen Ciurea, Costin Teodor Streba, Vlad Florin Iovanescu, Stefan Alexandru Artene, and Cristin Constantin Vere. Analysis of wireless capsule endoscopy images using local binary patterns. *Applied Medical Informatics*, 36(2):31, 2015.
15. Tsung-Chun Lee, Yu-Huei Lin, Noriya Uedo, Hsiu-Po Wang, Hsuan-Ting Chang, and Chung-Wen Hung. Computer-aided diagnosis in endoscopy: A novel application toward automatic detection of abnormal lesions on magnifying narrow-band imaging endoscopy in the stomach. In *35th Annual International Conference of the IEEE in Engineering in Medicine and Biology Society, EMBC*, pages 4430–4433, 2013.
16. Baopu Li, Max Q-H Meng, and James YW Lau. Computer-aided small bowel tumor detection for capsule endoscopy. *Artificial Intelligence in Medicine*, 52(1):11–16, 2011.
17. Farah Deeba, Francis M Bui, and Khan A Wahid. Computer-aided polyp detection based on image enhancement and saliency-based selection. *Biomedical Signal Processing and Control*, 55:101530, 2020.
18. Qian Wang, Ning Pan, Wei Xiong, Heng Lu, Nan Li, and Xijing Zou. Reduction of bubble-like frames using a RSS filter in wireless capsule endoscopy video. *Optics and Laser Technology*, 110(June 2018):152–157, 2019.
19. Davide Boschetto, Gianluca Di Claudio, Hadis Mirzaei, Rupert Leong, and Enrico Grisan. Automatic classification of small bowel mucosa alterations in celiac disease for confocal laser endomicroscopy. In *SPIE Medical Imaging*, volume 9788, pages 978809–978809. International Society for Optics and Photonics, 2016.
20. Michael Hafner, Toru Tamaki, Shinji Tanaka, Andreas Uhl, Georg Wimmer, and Shigeto Yoshida. Local fractal dimension based approaches for colonic polyp classification. *Medical Image Analysis*, 26(1):92–107, 2015.



References



21. Hirokazu Nosato, Hidenori Sakanashi, Eiichi Takahashi, and Masahiro Murakawa. Method of retrieving multi-scale objects from optical colonoscopy images based on image-recognition techniques. *IEEE Biomedical Circuits and Systems Conference: Engineering for Healthy Minds and Able Bodies, (BioCAS)*, pages 1–4, 2015.
22. Muhammad Attique Khan, Muhammad Rashid, Muhammad Sharif, Kashif Javed, and Tallha Akram. Classification of gastrointestinal diseases of stomach from wce using improved saliency-based method and discriminant features selection. *Multimedia Tools and Applications*, pages 1–28, 2019.
23. Sara Moccia, Gabriele O. Vanone, Elena De Momi, Andrea Laborai, Luca Guastini, Giorgio Peretti, and Leonardo S. Mattos. Learning-based classification of informative laryngoscopic frames. *Computer Methods and Programs in Biomedicine*, 158:21–30, 2018.
24. I. Sevo, A. Avramović, I. Balasingham, O. J. Elle, J. Bergsland, and L. Aabakken. Edge density based automatic detection of inflammation in colonoscopy videos. *Computers in Biology and Medicine*, 72:138–150, 2016.
25. Shuai Wang, Yang Cong, Jun Cao, Yunsheng Yang, Yandong Tang, Huaici Zhao, and Haibin Yu. Scalable gastroscopic video summarization via similar-inhibition dictionary selection. *Artificial Intelligence in Medicine*, 66:1–13, 2016.
26. Yang Cong, Shuai Wang, Ji Liu, Jun Cao, Yunsheng Yang, and Jiebo Luo. Deep sparse feature selection for computer aided endoscopy diagnosis. *Pattern Recognition*, 48:907–917, 2015.
27. Qian Zhao, Gerard E Mullin, Max Q-H Meng, Themistocles Dassopoulos, and Rajesh Kumar. A general framework for wireless capsule endoscopy study synopsis. *Computerized medical imaging and graphics*, 41:108–16, 2015.
28. Ahmed Z. Emam, Yasser A. Ali, and Mohamed M. Ben Ismail. Adaptive features extraction for Capsule Endoscopy (CE) video summarization. In *International Conference on Computer Vision and Image Analysis Applications, ICCVIA*, 2015.
29. Ali Yasar, Ismail Saritas, and Huseyin Korkmaz. Computer-Aided Diagnosis System for Detection of Stomach Cancer with Image Processing Techniques. *Journal of Medical Systems*, 43(4), 2019.
30. Yongsheng Dong, Huangbin Wu, Xuelong Li, Chuanqi Zhou, and Qingtao Wu. Multiscale Symmetric Dense Micro-Block Difference for Texture Classification. *IEEE Transactions on Circuits and Systems for Video Technology*, 2018.



References

31. Chun-Rong Huang, Yan-Ting Chen, Wei-Ying Chen, Hsiu-Chi Cheng, and BorShyang Sheu. Gastroesophageal Reflux Disease Diagnosis Using Hierarchical Heterogeneous Descriptor Fusion Support Vector Machine. *IEEE Transactions on Biomedical Engineering*, PP(99):1, 2015.
32. Yang Cong, Shuai Wang, Baojie Fan, Yunsheng Yang, and Haibin Yu. UDSFS: Unsupervised deep sparse feature selection. *Neurocomputing*, 2015.
33. Olga Dunaeva, Herbert Edelsbrunner, Anton Lukyanov, Michael Machin, and Daria Malkova. The classification of endoscopy images with persistent homology. In *16th International Symposium on Symbolic and Numeric Algorithms for Scientific Computing, SYNASC*, pages 565–570. Elsevier, 2015.
34. Yixuan Yuan, Jiaole Wang, Baopu Li, and Max Q H Meng. Saliency Based Ulcer Detection for Wireless Capsule Endoscopy Diagnosis. *IEEE Transactions on Medical Imaging*, 34(10):2046–2057, 2015.
35. Zhihong Zhang, Lu Bai, Peng Ren, and Edwin R. Hancock. High-order graph matching kernel for early carcinoma EUS image classification. *Multimedia Tools and Applications*, pages 1–20, 2015.
36. Jumpei Yamaguchi, Akihiko Yoneyama, and Teruya Minamoto. Automatic detection of early esophageal cancer from endoscope image using fractal dimension and discrete wavelet transform. In *12th International Conference on Information Technology-New Generations, (ITNG)*, pages 317–322. IEEE, 2015.
37. Roland Kwitt, Andreas Uhl, Michael Hafner, Alfred Gangl, Friedrich Wrba, and Andreas Vecsei. Predicting the histology of colorectal lesions in a probabilistic framework. In *IEEE Computer Society Conference on Computer Vision and Pattern Recognition Workshops (CVPRW)*, pages 103–110, 2010.
38. Michael Hafner, Leonhard Brunauer, Hannes Payer, Robert Resch, Alfred Gangl, Andreas Uhl, Friedrich Wrba, and Andreas Vecsei. Computer-aided classification of zoom-endoscopic images using fourier filters. *IEEE Transactions on Information Technology in Biomedicine*, 14(4):958–970, 2010.
39. M. Hafner, A. Gangl, M. Liedlgruber, A. Uhl, A. Vecsei, and F. Wrba. Combining Gaussian Markov random fields with the discretewavelet transform for endoscopic image classification. In *16th International Conference on Digital Signal Processing, DSP*, pages 1–6, 2009.
40. Fons Van Der Sommen, Sander R Klomp, Anne-fre Swager, Svitlana Zinger, Wouter L Curvers, Jacques J G H M Bergman, Erik J Schoon, and Peter H N De With. Computerized Medical Imaging and Graphics Predictive features for early cancer detection in Barrett's esophagus using Volumetric Laser Endomicroscopy. *Computerized Medical Imaging and Graphics*, 67(January):9–20, 2018.

References

41. Ahnaf Rashik Hassan and Mohammad Ariful Haque. Computer-aided gastrointestinal hemorrhage detection in wireless capsule endoscopy videos. *Computer Methods and Programs in Biomedicine*, 122(3):341–353, 2015.
42. Nimisha Elsa Koshy and Varun P Gopi. A new method for ulcer detection in endoscopic images. In *2nd International Conference on Electronics and Communication Systems (ICECS)*, pages 1725–1729. IEEE, 2015.
43. Farhan Riaz, Francisco Baldaque Silva, Mario Dinis Ribeiro, and Miguel Tavares Coimbra. Invariant gabor texture descriptors for classification of gastroenterology images. *IEEE Transactions on Biomedical Engineering*, 59(10):2893–2904, 2012.
44. Farhan Riaz, Miguel Areia, F Baldaque Silva, Mario Dinis-Ribeiro, P Pimentel’ Nunes, and M Coimbra. Gabor textons for classification of gastroenterology images. In *IEEE International Symposium on Biomedical Imaging: From Nano to Macro*, pages 117–120. IEEE, 2011.
45. Baopu Li and Max Q-H Meng. Texture analysis for ulcer detection in capsule endoscopy images. *Image and Vision Computing*, 27(9):1336–1342, 2009.
46. Michael Hafner, Roland Kwitt, Andreas Uhl, Alfred Gangl, Friedrich Wrba, and Andreas Vecsei. Feature extraction from multi-directional multi-resolution image transformations for the classification of zoom-endoscopy images. *Pattern Analysis and Applications*, 12(4):407–413, 2009.
47. Xiaodong Ji, Tingting Xu, Wenhua Li, and Liyuan Liang. Study on the classification of capsule endoscopy images. *EURASIP Journal on Image and Video Processing*, 2019(1):55, 2019.
48. Mark H. A. Janse, Fons van der Sommen, Svitlana Zinger, Erik J. Schoon, and Peter H. N. de With. Early esophageal cancer detection using RF classifiers. *Proc. SPIE 9785*, 9785:97851D–1 to 8, 2016.
49. An approach based on Fourier descriptors and decision trees to perform presumptive diagnosis of esophagitis for educational purposes, 2016.
50. Mekha Mathew and Varun P. Gopi. Transform based bleeding detection technique for endoscopic images. *2nd International Conference on Electronics and Communication Systems, ICECS*, pages 1730–1734, 2015.

References

51. F. van der Sommen, S. Zinger, E. J. Schoon, and P. H N de With. Supportive automatic annotation of early esophageal cancer using local gabor and color features. *Neurocomputing*, 144:92–106, 2014.
52. Hussam Ali, Muhammad Sharif, Mussarat Yasmin, and Mubashir Husain Rehmani. Importance of color descriptors for detection of gastric abnormalities from chromoendoscopy frames. *Biomedical Signal Processing and Control*, 2019.
53. Hussam Ali, Mussarat Yasmin, Muhammad Sharif, and Mubashir Husain Rehmani. Computer assisted gastric abnormalities detection using hybrid texture descriptors for chromoendoscopy images. *Computer Methods and Programs in Biomedicine*, 157:39–47, 2018.
54. Ruwan Nawarathna, JungHwan Oh, Jayantha Muthukudage, Wallapak Tavanapong, Johnny Wong, Piet C. de Groen, and Shou Jiang Tang. Abnormal image detection in endoscopy videos using a filter bank and local binary patterns. *Neurocomputing*, 144:70–91, 2014.
55. Sae Hwang and M. Emre Celebi. Polyp Detection in Wireless Capsule Endoscopy Video Based on Image Segmentations and Geometric Feature. In *IEEE International Conference on Acoustics Speech and Signal Processing, (ICASSP)*, volume 7, pages 678–681, 2010.
56. Alexandros Karargyris and Nikolaos Bourbakis. Identification of polyps in wireless capsule endoscopy videos using Log Gabor filters. In *IEEE/NIH Life Science Systems and Applications Workshop, LiSSA*, pages 143–147, 2009.
57. Farhan Riaz, Ali Hassan, Rida Nisar, Mario Dinis-Ribeiro, and Miguel Tavares Coimbra. Content-adaptive region-based color texture descriptors for medical images. *IEEE Journal of Biomedical and Health Informatics*, 21(1):162–171, 2017.
58. Shuai Wang, Yang Cong, Huijie Fan, Lianqing Liu, Xiaoqiu Li, sheng Yang, Yandong Tang, Huaici Zhao, and haibin Yu. Computer-Aided Endoscopic Diagnosis Without Human Specific Labeling. *IEEE Transactions on Biomedical Engineering*, 9294:1–1, 2016.
59. Rie Miyaki, Shigeto Yoshida, Shinji Tanaka, Yoko Kominami, Yoji Sanomura, Taiji Matsuo, Shiro Oka, Bisser Raytchev, Toru Tamaki, Tetsushi Koide, Kazufumi Kaneda, Masaharu Yoshihara, and Kazuaki Chayama. A computer system to be used with laser-based endoscopy for quantitative diagnosis of early gastric cancer. *Journal of Clinical Gastroenterology*, 49(2):108–115, 2015.
60. Yixuan Yuan, Baopu Li, and Qinghu Meng. Bleeding Frame and Region Detection in the Wireless Capsule Endoscopy Video. *IEEE Journal of Biomedical and Health Informatics*, 2194:1–1, 2015.

References

61. Limamou Gueye, Sule Yildirim-Yayilgan, Faouzi Alaya Cheikh, and Ilango Balasingham. Automatic detection of colonoscopic anomalies using capsule endoscopy. In *IEEE International Conference on Image Processing (ICIP)*, pages 1061–1064, 2015.
62. Barbara Andre, Tom Vercauteren, Aymeric Perchant, Anna M. Buchner, Michael B. Wallace, and Nicholas Ayache. Introducing space and time in local feature-based endomicroscopic image retrieval. *Lecture Notes in Computer Science (including subseries Lecture Notes in Artificial Intelligence and Lecture Notes in Bioinformatics)*, 5853 LNC:18–30, 2010.
63. Toshiaki Hirasawa, Kazuharu Aoyama, Tetsuya Tanimoto, Soichiro Ishihara, Satoki Shichijo, Tsuyoshi Ozawa, Tatsuya Ohnishi, Mitsuhiro Fujishiro, Keigo Matsuo, Junko Fujisaki, et al. Application of artificial intelligence using a convolutional neural network for detecting gastric cancer in endoscopic images. *Gastric Cancer*, pages 1–8, 2018.
64. Jun-Yan He, Xiao Wu, Yu-Gang Jiang, Qiang Peng, and Ramesh Jain. Hookworm Detection in Wireless Capsule Endoscopy Images with Deep Learning. *IEEE Transactions on Image Processing*, 27(5):1–1, 2018.
65. Ruikai Zhang, Yali Zheng, Tony Wing Chung Mak, Ruoxi Yu, Sunny H. Wong, James Y.W. Lau, and Carmen C.Y. Poon. Automatic Detection and Classification
66. of Colorectal Polyps by Transferring Low-Level CNN Features from Nonmedical Domain. *IEEE Journal of Biomedical and Health Informatics*, 21(1), 2017.
67. Emilio Garcia, Renato Hermoza, Cesar Beltran Castanon, Luis Cano, Miluska Castillo, and Carlos Castanneda. Automatic lymphocyte detection on gastric cancer ihc images using deep learning. In *IEEE 30th International Symposium on Computer-Based Medical Systems (CBMS)*, pages 200–204. IEEE, 2017.
68. Yang Nan, Gianmarc Coppola, Qiaokang Liang, Kunlin Zou, Wei Sun, Dan Zhang, Yaonan Wang, and Guanzhen Yu. Partial Labeled Gastric Tumor Segmentation via patch-based Reiterative Learning. *arXiv*, (December), 2017.
69. Jia-sheng Yu, Jin Chen, ZQ Xiang, and Yue-Xian Zou. A hybrid convolutional neural networks with extreme learning machine for wce image classification. In *IEEE International Conference on Robotics and Biomimetics (ROBIO)*, pages 1822–1827, 2015.
70. Yuexian Zou, Lei Li, Yi Wang, Jiasheng Yu, Yi Li, and W J Deng. Classifying digestive organs in wireless capsule endoscopy images based on deep convolutional neural network. In *IEEE International Conference on Digital Signal Processing (DSP)*, pages 1274–1278, 2015.
71. Guobing Pan, Guozheng Yan, Xiangling Qiu, and Jiehao Cui. Bleeding detection in wireless capsule Endoscopy based on probabilistic neural network. *Journal of Medical Systems*, 35:1477–1484, 2011.

References

- 72 <https://aidasub-chromogastro.grand-challenge.org/>
73 University of Aveiro, Portugal
74 <https://aidasub-cleceliacy.grand-challenge.org/>
75 <https://aidasub-clebarrett.grand-challenge.org/>
76 <https://endovissub-abnormal.grand-challenge.org>
77 <https://polyp.grand-challenge.org/>
78 <https://datasets.simula.no/kvasir/>
79 Farhan Riaz, Francisco Baldaque Silva, Mario Dinis Ribeiro, and Miguel Tavares Coimbra. Invariant gabor texture descriptors for classification of gastroenterology images. *IEEE Transactions on Biomedical Engineering*, 59(10):2893–2904, 2012.
80 Hussam Ali, Muhammad Sharif, Mussarat Yasmin, and Mubashir Husain Rehmani. Computer-based classification of chromoendoscopy images using homogeneous texture descriptors. *Computers in Biology and Medicine*, 88:84–92, September 2017.
81 Hussam Ali, Mussarat Yasmin, Muhammad Sharif, and Mubashir Husain Rehmani. Computer assisted gastric abnormalities detection using hybrid texture descriptors for chromoendoscopy images. *Computer Methods and Programs in Biomedicine*, 157:39–47, 2018.
82 Robert M Haralick, Karthikeyan Shanmugam, et al. Textural features for image classification. *IEEE Transactions on systems, man, and cybernetics*, 3(6):610–621, 1973.
83 Baopu Li and Max Q H Meng. Tumor recognition in wireless capsule endoscopy images using textural features and SVM-based feature selection. *IEEE Transactions on Information Technology in Biomedicine*, 16(3):323–329, 2012.
84 Samruddhi Y Kahu, Rajesh B Raut, and Kishor M Bhurchandi. Review and evaluation of color spaces for image/video compression. *Color Research & Application*, 44(1):8–33, 2019.
85 Shanwen Zhang, Haoxiang Wang, Wenzhun Huang, and Zhuhong You. Plant diseased leaf segmentation and recognition by fusion of superpixel, k-means and phog. *Optik*, 157:866–872, 2018.
86 Dana E Ilea and Paul F Whelan. Color image segmentation using a spatial k-means clustering algorithm. 2006.
87 Farhan Riaz, Francisco Baldaque Silva, Mario Dinis Ribeiro, and Miguel Tavares Coimbra. Impact of visual features on the segmentation of gastroenterology images using normalized cuts. *IEEE Transactions on Biomedical Engineering*, 60(5):1191–1201, 2013.
88 Wen Xiao, Aleksandra Zaforemska, Magdalena Smigaj, Yunsheng Wang, and Rachel Gaulton. Mean shift segmentation assessment for individual forest tree delineation from airborne lidar data. *Remote Sensing*, 11(11):1263, 2019.
89 Geming Wu, Xinyan Zhao, Shuqian Luo, and Hongli Shi. Histological image segmentation using fast mean shift clustering method. *Biomedical engineering online*, 14(1):24, 2015.
90 Vijay Badrinarayanan, Alex Kendall, and Roberto Cipolla. Segnet: A deep convolutional encoder-decoder architecture for image segmentation. *IEEE transactions on pattern analysis and machine intelligence*, 39(12):2481–2495, 2017.

Thank You



Questions and Answers

